NOTICE

The quality of this microform is heavily dependent upon the quality of the original thesis submitted for microfilming. Every effort has been made to ensure the highest quality of reproduction possible.

If pages are missing, contact the university which granted the degree.

Some pages may have indistinct print especially if the original pages were typed with a poor typewriter ribbon or if the university sent us an inferior photocopy.

Reproduction in full or in part of this microform is governed by the Canadian Copyright Act, R.S.C. 1970, c. C-30, and subsequent amendments.

AVIS

La qualité de cette microforme dépend grandement de la qualité de la thèse soumise au microfilmage. Nous avons tout fait pour assurer une qualité supérieure de reproduction.

S'il manque des pages, veuillez communiquer avec l'université qui a conféré le grade.

La qualité d'impression de certaines pages peut laisser à désirer, surtout si les pages originales ont été dactylographiées à l'aide d'un ruban usé ou si l'université nous a fait parvenir une photocopie de qualité inférieure.

La reproduction, même partielle, de cette microforme est soumise à la Loi canadienne sur le droit d'auteur, SRC 1970, c. C-30, et ses amendements subséquents.

Experimental Study of Wind Induced Suction on Flat Roofs

By

Samia Ghariani

A Thesis presented to the University of Ottawa in partial fulfillment of the requirements for the degree of Master of Applied Science in Civil Engineering

DEPARTMENT OF CIVIL ENGINEERING
UNIVERSITY OF OTTAWA
Ottawa, Ontario, Canada
April 1991

ISBN 0-315-70498-5

UNIVERSITÉ D'OTTAWA
UNIVERSITY OF OTTAWA

Abstract

A 1:10 scale model building previously tested in the NRCC $9m \times 9m$ wind tunnel was reproduced with a more exaggerated scale of 1:100 in a smaller wind tunnel and tested. Also tested was a half of the building cut along the line of symmetry and with various heights. The purpose of the testing was

1) to examine the repeatability of the roof pressure patterns with a more exaggerated scaling factors, and

2) to explore the feasibility of using a portion of the building for the testing of structural details against wind action.

It was confirmed that the proposed simulation of only a half or even less portion of the building at various scaling factors can be a useful wind tunnel testing method which can reproduce the previously established full building test results as long as the parapet height ratio is kept constant and the wind tunnel blockage ratio is kept minimal.

This thesis is dedicated to
my lovely parents and fiancé Aref

Acknowledgement

The auther wishes to express her special gratitude to Dr. H. Tanaka for his supervision, constructive advice and encouragement. Special appreciation is expressed to Dr. R. L. Wardlaw for his proposal and to Mr. K. Kimura for his help in the experimental work and to the NRCC and its staff without which she would not have been able to accomplish the experiment.

She would like also to express her sincere thanks to the Tunisian Government for its scholarship program.

Contents

Chapters

List of Tables

List of Figures

Notation

Various symbols and abreviations used frequently in this work are summarized below. All notation is fully defined where it first arises in the text.

Symbols

U	Mean wind speed
U_e	Reference wind speed
U'_e	Wind speed fluctuation
C_p	Mean pressure coefficient
h_p	Parapet height
h	Building height
h_p/h	Parapet ratio
B	Width of the building
L	Length of the building
S	Model area normal to the flow
C	Wind tunnel cross-sectional area
S/C	Blockage ratio

Abreviations

NRCC	National Research Council Canada
ANSI	American National Standards Institute

Chapter 1

Introduction

A flat roof surface often experiences very high suction induced by the pair of vortices from the upstream corner against the diagonal wind [1,2]. Since this phenomenon can cause serious dislocation of the roofing system such as insulation boards or concrete pavers, it is encouraged to mechanically fasten them to the roof deck rather than leaving them loose-laid [3]. However, once they are firmly connected to the roof deck, there still remains a possibility of inflation of the roof deck itself or even structural damages due to it because the building cannot be completely airtight and tends to allow air infiltration underneath the roof to allow this deformation [4,5].

Wind tunnel testing of this situation is difficult with a scaled model because the structural details can hardly be modelled both mechanically and geometrically in reduced scale. Wind tunnel testing of a full scale building, on the other hand, would be nearly impossible.

A proposal has been made to manipulate this situation suggesting the possibility of wind tunnel testing only a half or even smaller portion of the building which is still kept in nearly full scale using exceptionally large wind tunnel facilities. An important question here is whether or not we really have a good simulation of the reality in this way; i.e., the realization of extremely high suction due to wind when only a portion of the structure is modelled. Figs. 1.1 and 1.2 illustrate the idea of this testing method indicating the increase of the model scale when only a half-model with the same vortices developed in larger scale is tested.

What is presented here is a pilot study towards this interesting problem. A 1/10-scaled model of the building previously tested in the NRCC $9m \times 9m$ wind tunnel was constructed with a further reduction in scale to 1/100 in a smaller wind tunnel (the NRCC $0.9m \times 0.9m$ wind tunnel which is a 1/10 -scaled model of the $9m \times 9m$ tunnel) and was tested, first of all, to make sure that the same pressure pattern can be reproduced. Then the same model was reduced its configuration from a full building to only a half of it to examine if the wind induced pressure pattern in the critical area of the roof would remain the same. Finally this portion of the roof was reproduced in much larger scales (1/37.5 and 1/21) to occupy larger area of the wind tunnel to see if test results remain the same.

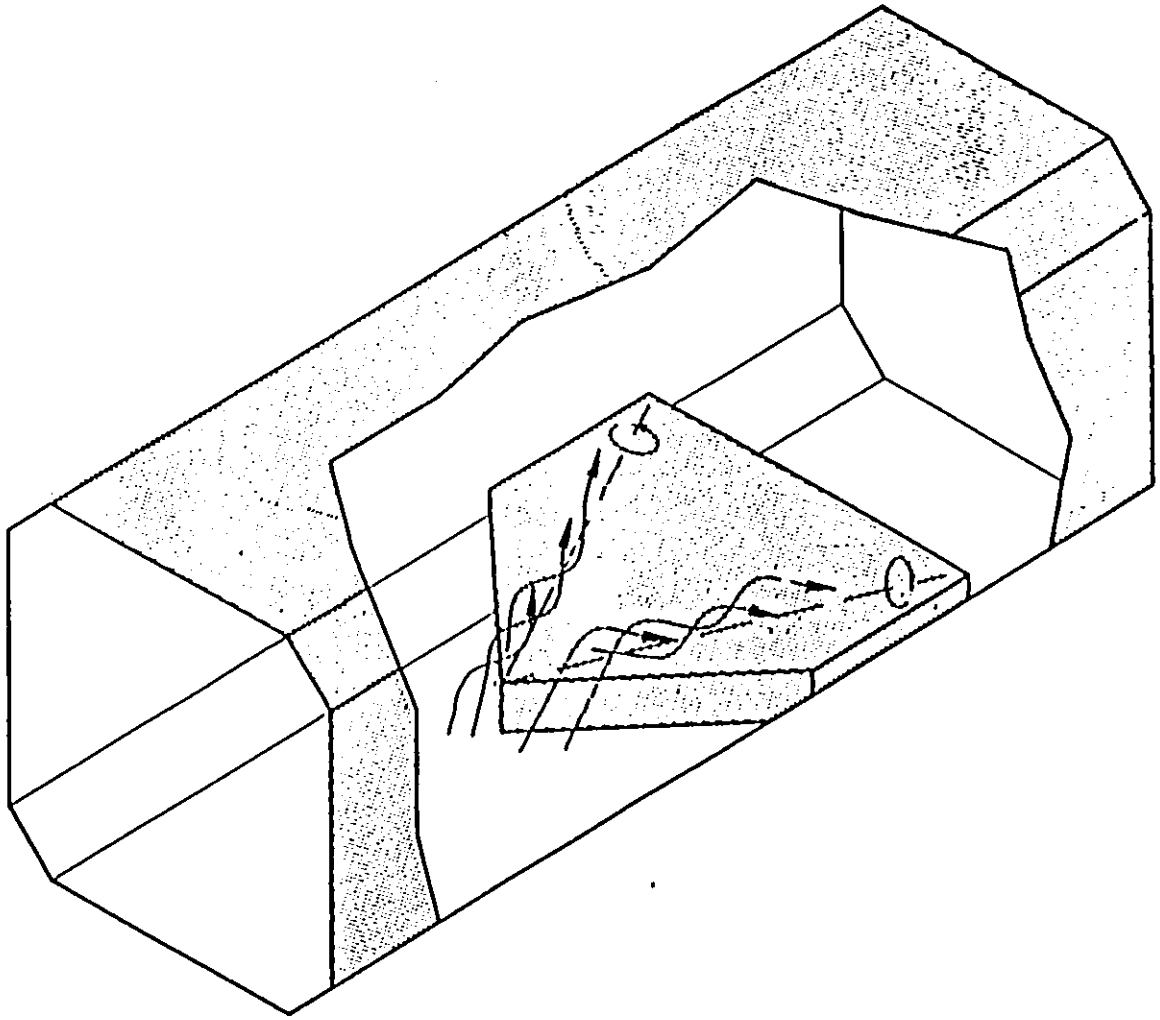

Figure 1.1: Concept of the Model in Wind Tunnel

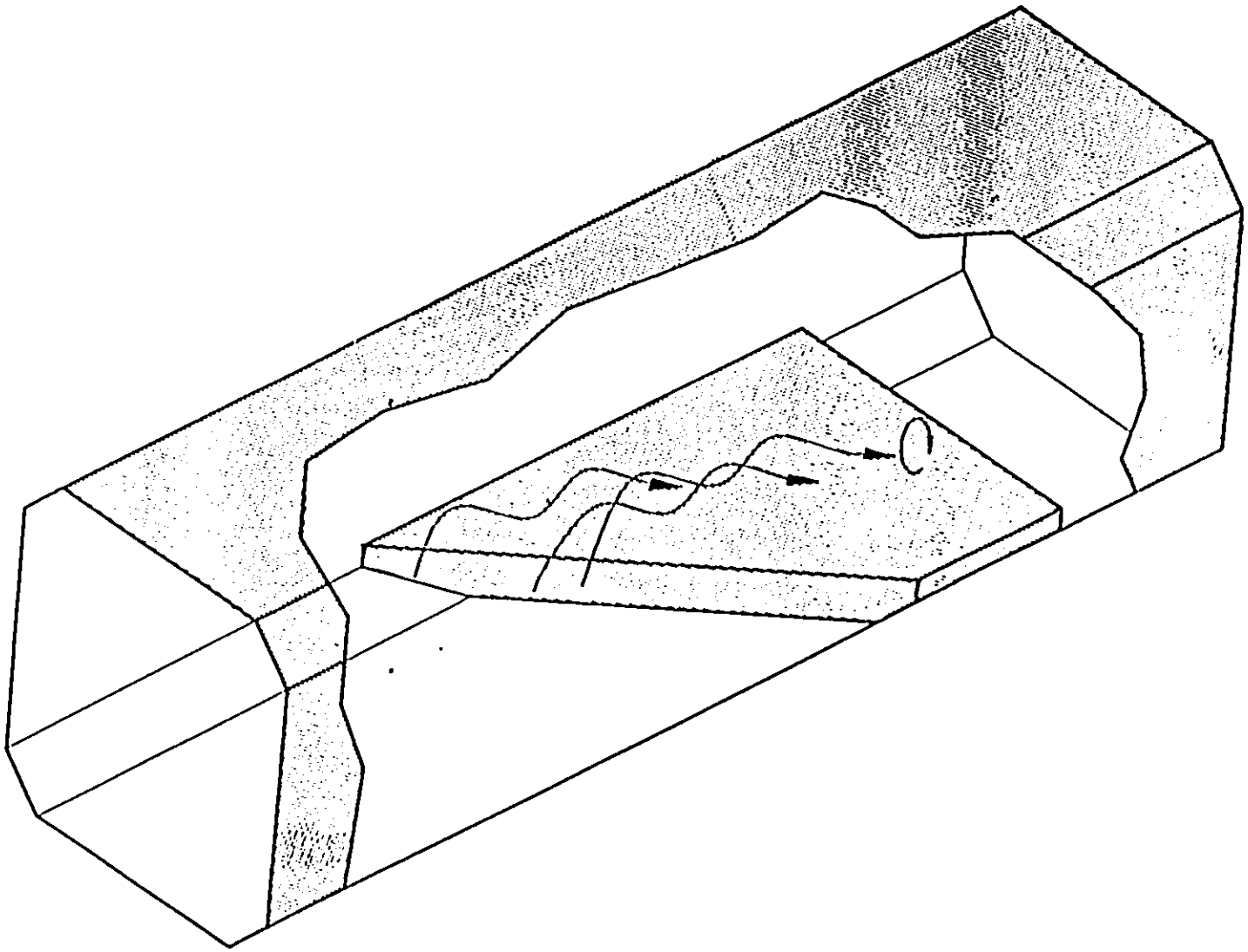

Figure 1.2: Concept of a Half-Model in Wind Tunnel

The purpose of this series of testing is very simple. The idea is that if the final stage of the test would still give the same experimental results, a very large building model with the linear scale of 1/2 or even 1/1 can be installed in the $9m \times 9m$ wind tunnel, which makes it easier to examine the effectiveness of the structural details against the anticipated strong wind action.

Even when the building model is constructed in such a scale, the building height cannot be simulated with the same linear scale because the wind tunnel blockage becomes too excessive. However if the building height is reduced, the resulted roof pressure may not be the same and a correction is needed for height effect and/or blockage effect.

Another question related to this, is the height of the parapet. It has been known that the parapet height has an important influence on the roof pressure simulation [6]. These additional three factors i.e parapet effect, height effect and blockage effect, are also considered in this study.

Chapter 2

Literature Review

Wind induced pressure can cause various types of problems on building structures. In particular it has been recognized for a long time that a flat roof is subjected to very high suction caused by vortices generated at the upstream corner [1,2].

These vortices are most severe with diagonal wind of 45° direction where strong vortices form along both diagonal edges of the rooftop which amplify the wind speed and then area under the vortices is subjected to large aerodynamic uplift [3,]. This phenomenon has caused serious damages. Despite of some attempts made in the past to solve this problem, more concern should be paid to the wind effect in the design of flat roof buildings.

2.1 Full Scale Observations

According to the recent development of the research towards this problem, these damages are mainly described as follows:

- Gravel scour from the rooftop and the damage on neighboring buildings and cars caused by flying gravel missiles. Fig. 2.1 shows the roof gravel scour on building roofs [7,8].

- Serious dislocation of roofing system such as insulation boards and concrete pavers. The loss of roofing material can further cause damages on interiors of the property . Fig. 2.2 shows damage to an architectural metal roof [7].

2.2 Wind Tunnel Tests

2.2.1 Suction on Flat Roofs in General

In modern roofing systems, elements, as insulation boards or concrete pavers are usually placed on the impermeable membrane of the roof. Usually, these slabs are loose-laid and are not mechanically fastened to the roof deck. Such elements can be dislocated by strong wind, as proved by experiments [3], at wind direction of 45° where strong vortices are created. Those vortices cause the critical situation at the upwind corner where highly spatial variations

of static pressure occur.

Replacing gravel by a layer of boards or pavers has not solved the problem entirely though the failure mechanisms have been proved to be very different in these cases. In the case of gravel, there is airflow all around a given stone so that aerodynamic forces can cause stone movement [5,9,10]. In the case of pavers or boards, on the other hand, they form a flat surface and the airflow is basically just over the top of this surface. Little aerodynamic lift force can be developed to cause saltation for this case. However, recent studies have shown that the dislocation of these pavers or boards can be caused by the strong suction on their exterior and underneath surfaces developed as a result of wind action [3,4,11].

The problem of dislocation of roofing systems and damages is still present whichever the cause is, and the damage can even be more severe in the case of paving slabs or board displacement than in the case of gravel blowoff. R.J.Kind and R.L.Wardlaw, after studying the failure mechanisms of loose-laid insulation systems, recommended to fasten them to the roofdeck rather than leaving them loose-laid [3]. However, the experiments have shown that once they are connected to the roofdeck, even the whole roof can be inflated and this, of course, will cause structural damages since the system is not impermeable and the air infiltration will transmit the high suction wind pressure underneath the roof to allow this deformation[4,5].

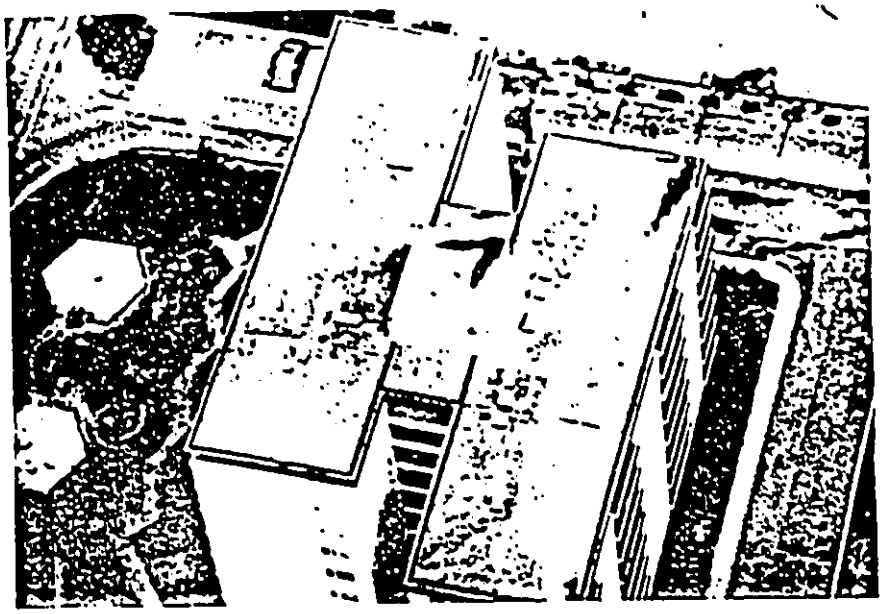

Example of Full Scale Stone Scour [8]

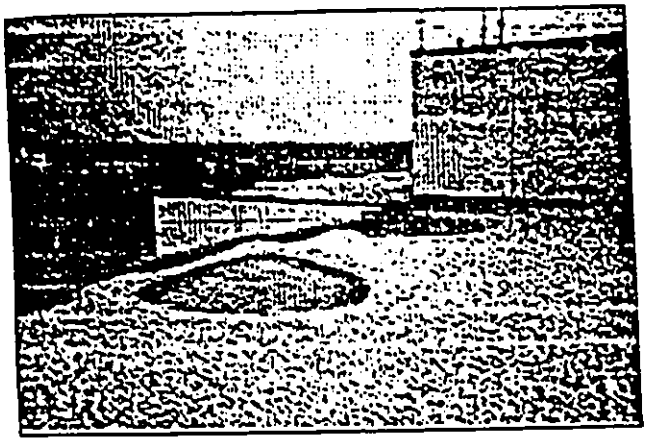

Roof gravel scour from the roof of the Trident Hospital Charleston [7]

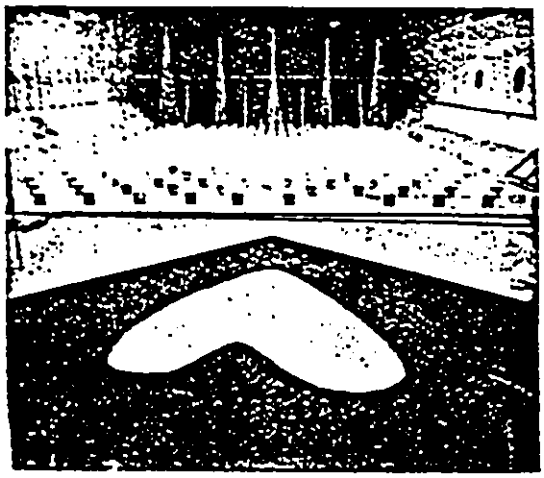

Typical Scour Pattern on Square Planform Low-Rise Building [8]

Figure 2.1: Examples of Gravel Scour

Damage to an architectural metal roof during Hurricane Hugo [7]

Figure 2.2: Damage to a Metal Roof

2.2.2 Effect of Parapets

Leutheusser (1964):

"The effect of wall parapets on the roof pressure coefficients of block type and cylindrical structures"[12]

Parapets cause a drastic reduction of the high suction, particularly at the corners and edges of the roof, for oblique wind directions. Leutheusser summarized his conclusions as follows :

It must be emphasized that the only benefit with regard to roof wind loading derivable from the use of parapets concerns their effect in making the roof pressure distribution more uniform. Both the magnitude of the average roof pressure coefficient -the net uplifting force- and the pressure distribution over the building side walls are affected by the presence of parapet. Thus pertinent design information listed in the building codes for flat roofed structures without parapets applies unchanged also to these buildings.

Fig. 2.3 shows results of his study.

Columbus (1972):

"The study of pressure coefficients on large flat roofs and the effects of parapets on these coefficients" [13]

Columbus's results obtained in uniform flow confirmed Leutheusser's data but tests in turbulent flow indicated that parapets do not cause any reduction of mean pressure coefficients.

Kind (1974):

"Gravels blown off rooftops"[1]

The critical wind speeds at which gravels are blown off rooftops increase by increasing the parapet height and decrease by increasing the building height, which implies that parapets reduce the pressure coefficients on the roof.

Davenport and Surry (1974):

"Effects of parapets on the wind loads of low-rise buildings"[14]

Low parapets on low buildings may lead to even more severe local suction than that for a plain flat roof.

Kramer et al. (1978):

"Effect of parapets on the wind loads of flat roofs"[15]

Parapets change the pressure coefficients significantly only on the corner regions of the roof. Fig. 2.4 illustrates that for square buildings, only low parapets of low buildings may cause some increase on mean pressure coefficients acting on roof corners. Peak values of pressure coefficients are always reduced by parapets.

Sockel and Tancher (1980):

"Measurement of mean and extreme pressure coefficients on points close to the roof corner"[16]

A parapet height equal to approximately 2% of the height of the building reduces both mean and peak suction by as high as 50% in its magnitude.

Stathopoulos (1982):

"Effect of parapets on low buildings"[17]

As shown from Fig. 2.5 [34], the parapet causes a reduction of edge wind

loads but it increases both mean and peak suction on roof corners. In this study it needs to note that only one parapet height (1.2 m) was examined.

Lythe and Surry (1983):

"Model study in a simulated boundary layer in a wind tunnel"[18]

Peak pressures in the edge regions are found to be reduced by parapets. Mean pressures in the edge region are found to be increased by parapets on low roofs and decreased on high roofs. It should be noted that this study has its special concern on relatively low buildings and only parapet height greater than 1.3 m in full scale were tested

Stathopoulos and Baskaran (1987-1988):

"Wind pressures on flat roofs with parapets "[19]

"Turbulent wind loading of roofs with parapet configurations"[20]

Stathopoulos and Baskaran examined, the effect of wind on a variety of flat roofs with and without parapets for a variety of wind directions and showed that parapets generally reduce the high suction on roof edges and may slightly increase the suction on the interior areas of the roof, the roof-corner suction, however, was found to increases significantly for low parapet heights. This contradicts the ANSI provisions for the effect of parapets on roof suction. This point will be discussed again in later chapter.

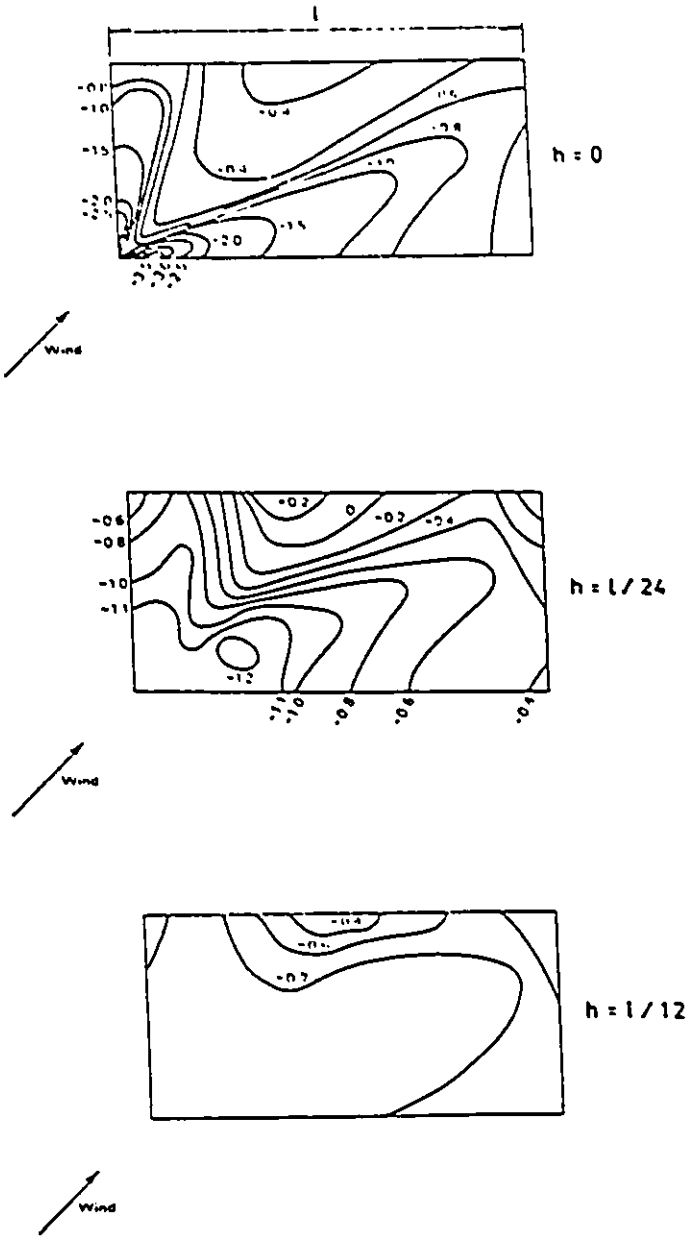

Effect of parapet on mean pressure coefficient distribution
a roof with oblique wind incidence

Figure 2.3: Results of Leutheusser study(19C4)

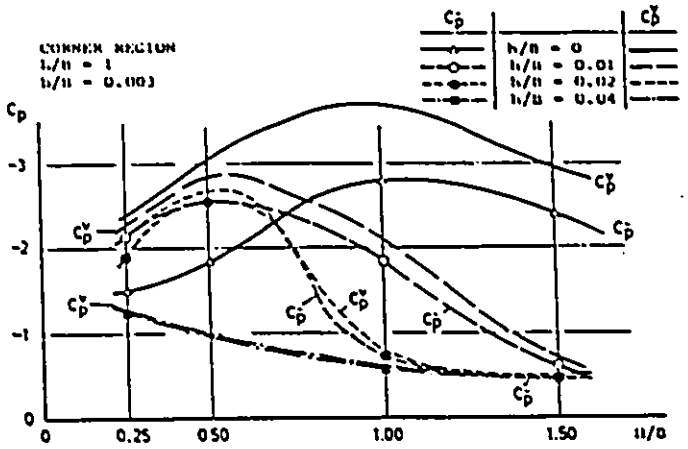

Influence of parapets on wind pressure coefficients for corner regions of flat roofs (after Kramer *et al.* 1978).

Figure 2.4: Results of Kramer et al. study(1978)

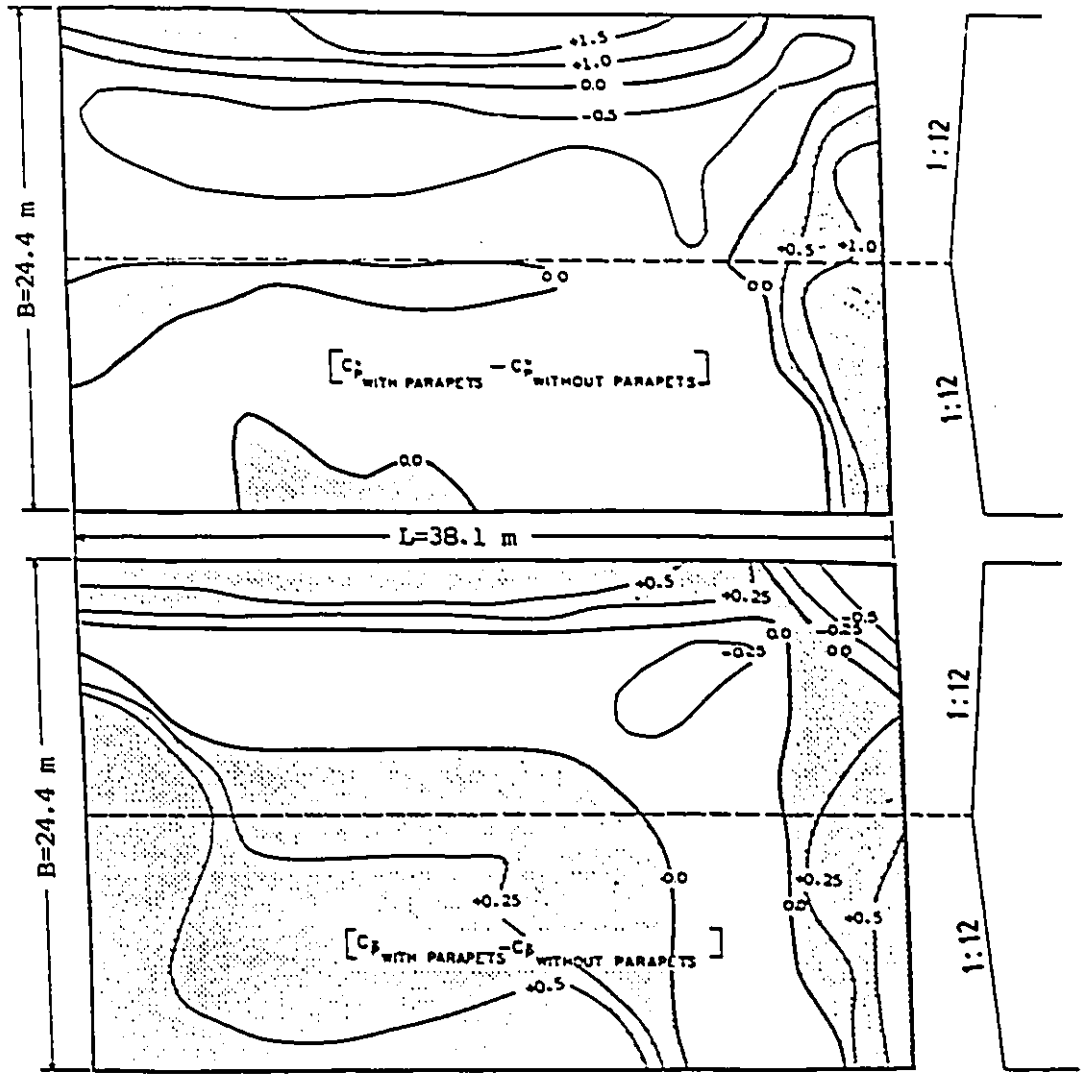

Contours of roof local pressure coefficient differenes for buildings with and without parapets—shading indicates reduction of wind loads for low building with parapets (after Stathopoulos 1982).

Figure 2.5: Results of Stathopoulos study(1982)

In conclusion, the use of parapets is said to result the followings :

- A drastic reduction of suction at the corners and edges.
- A reduction of suction in uniform flow but no reduction on mean pressure coefficients in turbulent flow.
- Increase in suction with low parapet.
- A significant change only in the corner pressure coefficient.
- Increase of roof corners mean pressure coefficient.
- A reduction of peak pressure coefficients.
- Reduction of both mean and peak suctions.
- A reduction on edges but an increase of suction on corners.
- A reduction of peak pressure in the edge.
- An increase of mean pressure in edges.
- Increase of both mean and peak suctions at corner region.
- A slight increase of suction on interior areas.

Some of the above statements obviously contradict each other. It is partly caused by the fact that not all of these studies specify all the parameters clearly, or even if they are specific, the results may have been influenced by interaction of parameters. This will be reviwed again in Chapt.5.

Chapter 3

Experimental Investigation

3.1 Facilities

The experiments were conducted at the 0.9m×0.9m wind tunnel of the Low Speed Aerodynamics Laboratory, currently renamed as the Applied Aerodynamics Laboratory, National Research Council Canada.

The air flow at the 2.2m test section of the wind tunnel was set to be a turbulent boundary layer of about 0.38m deep with the power law exponent of approximately 0.26. The profile of longitudinal turbulence intensity is shown in Fig. 3.1.

This boundary layer was created by installing the spires of 35 cm high at the upstream end of the test section in order to simulate the flow characteristics of the assumed natural wind . The mean velocity profile is shown in Fig. 3.2.

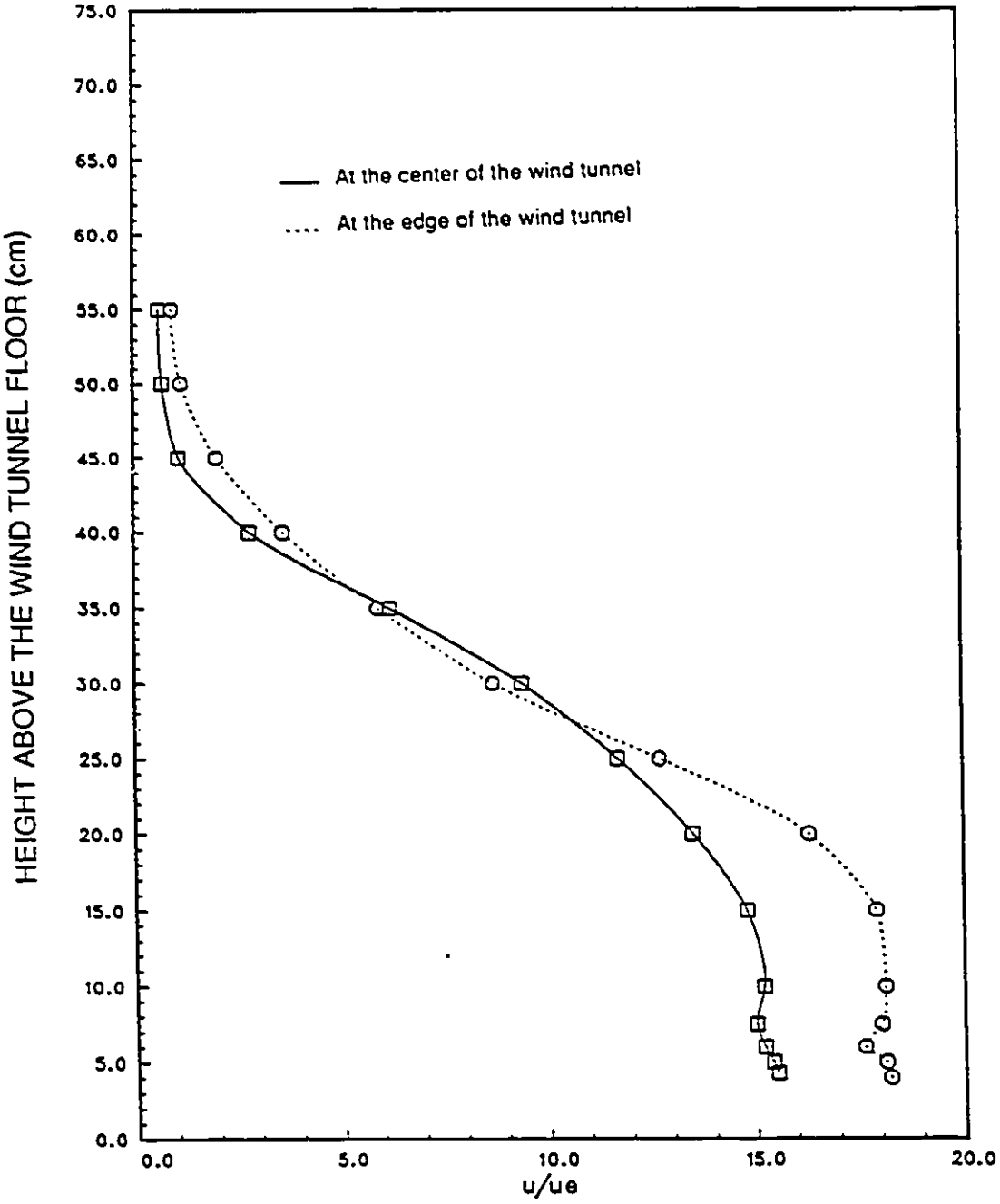

Figure 3.1: Profile of Longitudinal Turbulence Intensity

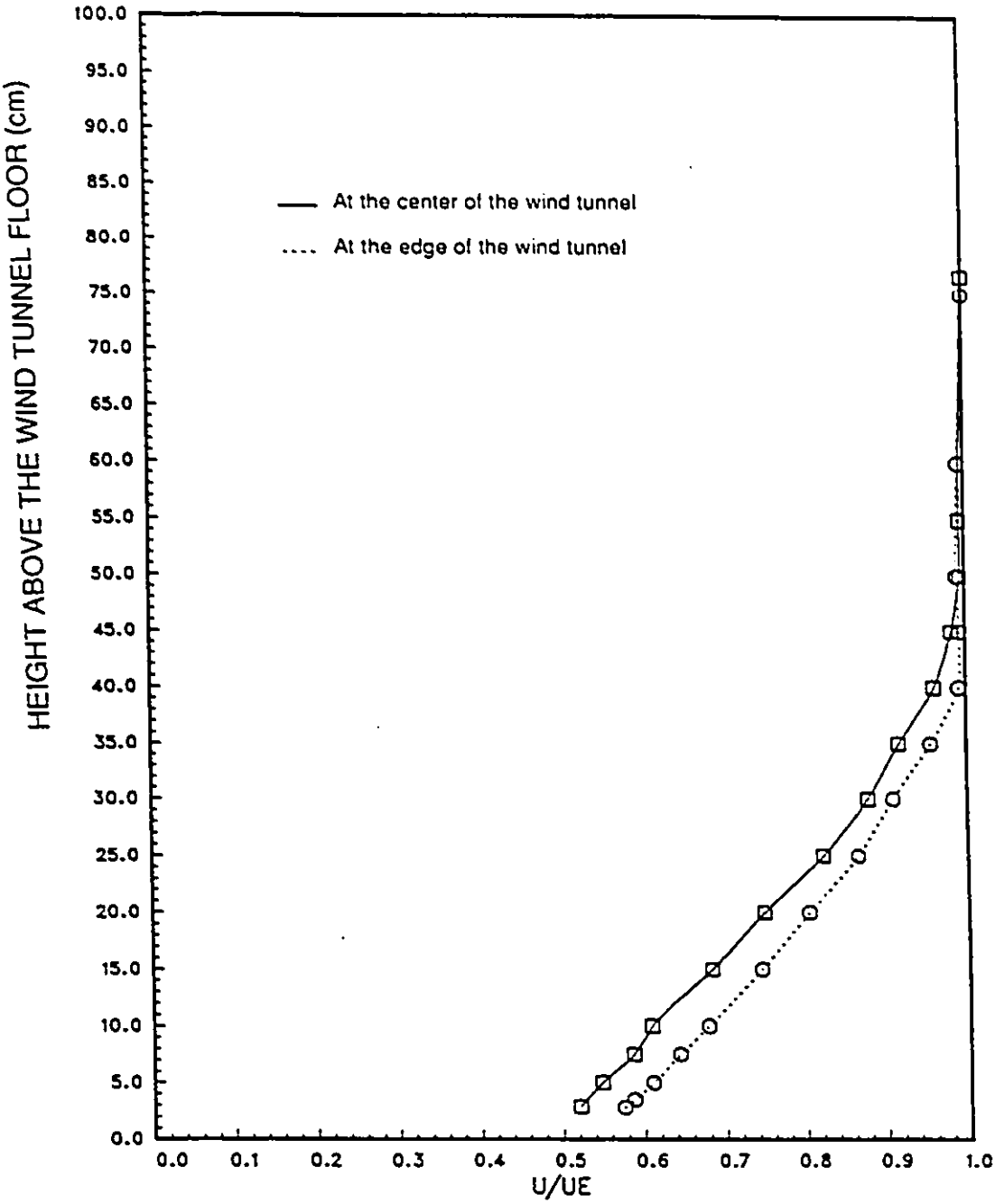

Figure 3.2: Mean Velocity Profile

3.2 Similitude Requirements

If the model tests are to be meaningful, conditions must be such that the model behavior is dynamically similar to that of the prototype [21]. Dimensional analysis and similarity considerations indicate that this will be achieved, if the wind approaching the model satisfactorily simulates the natural wind, if all model dimensions are correctly scaled and if the Reynolds number, Froude number and density ratio have the same numerical values in both the model and prototype situations.

Simulation requirements for this test can be summarized as follows :

3.2.1 Dynamic Simulation

Both Reynolds number (VL/ν)and Froude number ($V/\sqrt{LG}$) are two major factors for fluid dynamic simulation requirements, where V is the reference wind speed which is taken at roof top elevation for this test, L is the reference length such as the building height, G is the gravitational acceleration and ν is the kinematic viscosity of the air.

Froude similitude leads to the following equation :

$$(V^2/LG)_p = (V^2/LG)_m \Rightarrow V_p = V_m\sqrt{(L_p/L_m)} \tag{3.1}$$

Reynolds similitude leads to the following equation :

$$(VL/\nu)_p = (VL/\nu)_m \Rightarrow V_p = V_m(L_m/L_p)(\nu_p/\nu_m) \qquad (3.2)$$

The suffixes "p" and "m" stand for "prototype" and "model" respectively. These two equations lead us to the conclusion that it is impractical to satisfy both similitude requirements simultaneously. Since the nature of the experiment seems to be less dependent upon Reynolds number, the choice for this case is to relax Reynolds number similitude requirement. Fortunately, the previous tests [8,22] have shown that the main characteristics of the flow which create the pressure pattern over the upwind corner of the flat roof of the building can be obtained without satisfying the Reynolds number requirements. Froude similitude is then considered to be the guide line.

3.2.2 Geometric Simulation

The prototype building of 24m×24m×4.5m with a parapet height of 0.15m referred to in the ref.[3] is again used as the prototype building in this study. The linear scaling factors used for this study are 1/100, 1/37.5 and 1/21.

The scaling factor of 1/100 was chosen as 1/10 of the previously tested model at the 9m × 9m wind tunnel since the wind tunnel used this time was a 1/10 of the 9m × 9m tunnel. The middle scale, 1/37.5, was decided by spreading the whole diagonal length of the building to cover the width of the wind tunnel test section which is 0.90m.

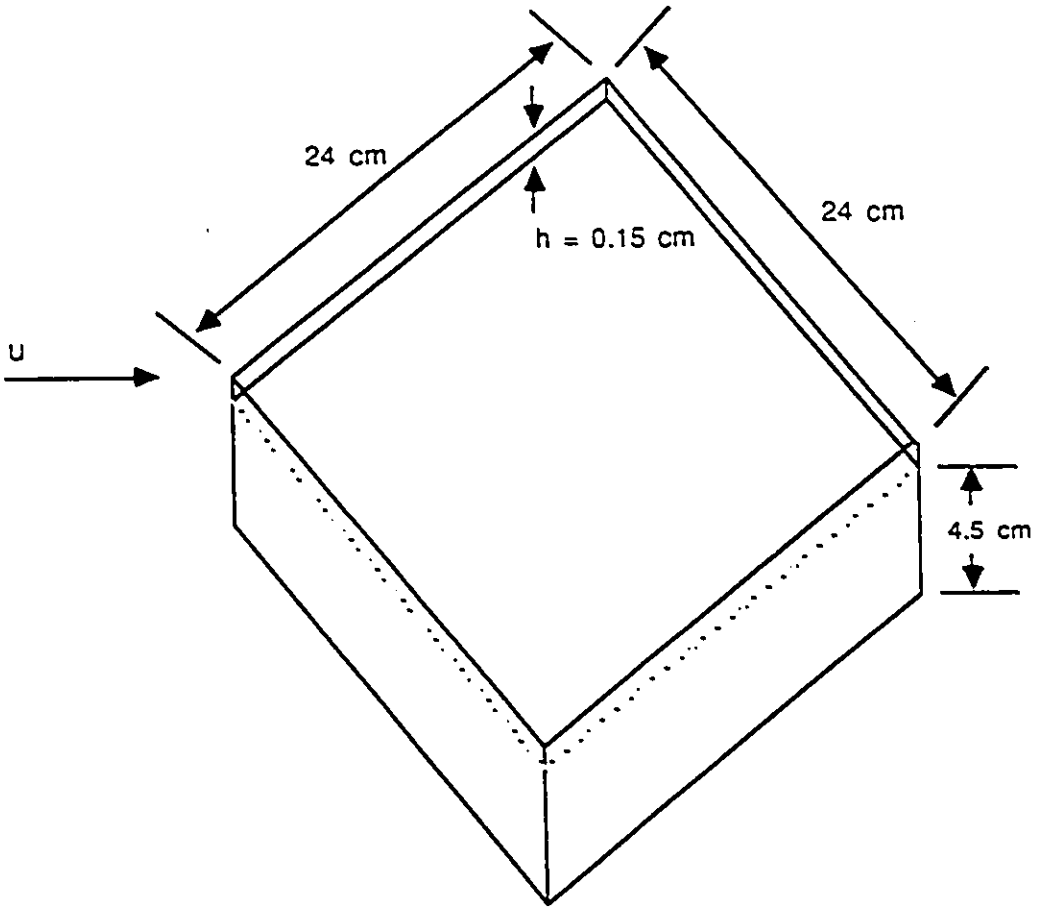

Figure 3.3: Sketch of the 1/100 Model Building

The original choice of the largest model was to make an expanded model of a half of the 1/37.5 scaled model to the maximum size the wind tunnel can accommodate. By doing so, the most upstream tip of the building will come right on the wind tunnel wall. Because of a consideration that there may be thin boundary layers unintentionally developed on both walls of the wind tunnel, it was decided that the above mentioned situation should be avoided. The last scaling factor of 1/21 was thus chosen to locate the building tip slightly away from the wall.

3.3 Models

The scales, dimensions and configuration of the models tested are summarized in Table 3.1.

In naming the models, the first letter designates the model size; A for small, B for medium and C for large. The second letter designates the height of the model; L for low and H for high models. The third letter designates the building configuration; W for a whole building and H for a half model of the structure. For example, the model ALW is a small model (scale 1/100) of the whole building with the lowest parapet equivalent to 15cm in full scale.

Table 3.1: List of models tested

Symbols	Scale	Side length (cm)	Height (cm)	Blockage (%)	Parapet height (cm)	Parapet ratio	Configuration
	full	24m	4.5m		15cm	.0330	
ALW	1/100	24	4.5	1.8	.15	.0330	whole
ALH	1/100	24	4.5	0.9	.15	.0330	half
ALHP	1/100	24	4.5	0.9	.15	.0330	half
AMW	1/100	24	9.0	3.7	.15	.0170	whole
AHW	1/100	24	12.0	4.9	.15	.0125	whole
BHW	1/37.5	64	12.0	13.0	.40	.0330	whole
BLW	1/37.5	64	4.5	4.9	.40	.0890	whole
BLHPL	1/37.5	64	4.5	2.4	.40	.0890	half
BLHPH	1/37.5	64	4.5	2.4	.40	.0890	half
CL	1/21	115	4.5	4.9	.72	.1600	half
CH	1/21	115	21.6	24.0	.72	.0330	half

- The model ALW (Fig. 3.4) is a 1/100-model of the assumed prototype building. It represents also a 1/10-model of what was previously tested at the NRCC 9m × 9m wind tunnel [3] which itself is a 1/10-model of the full scale building. Since both the model and wind tunnel are reduced in this experiment to 1/10 in linear scale compared to the previous testing, the measured pressure pattern is expected to be the same as the previous one.

- The model ALH (Fig. 3.5) is a half-building configuration of ALW with the same linear scale. Since the model and flow conditions for ALW are considered to be symmetric with respect to the wind tunnel centerline, and indeed the pressure results are known to be almost symmetric, it was investigated if the same pressure pattern can be produced by having only a half of the model.

- The model ALHP (Fig. 3.6) is the same as ALH except a vertical plate is attached in longitudinal direction along the diagonal cut of the building trying to better ensure the two-dimensionality of the flow.

- The model BHW (Fig. 3.7) is the same as ALW except the linear scale is now 1/37.5 rather than 1/100. The model occupies the whole wind tunnel width and the blockage ratio is increased to 13%. This rather substantial blockage might influence the pressure distribution pattern on the model.

- The model BLW (Fig. 3.8) is a reduced height model in order to reduce

the problem of blockage. However, for this case, the ratio of parapet height to the building height is nearly trippeled which would certainly influence the pressure results.

- The models BLHPL and BLHPH (Fig. 3.9 and 3.10) are half-building configuration models similar to BLW with a low plate for BLHPL and a higher plate for BLHPH placed in the same way as in ALHP

- The model CH (Fig. 3.11) is a 1/21 model. The line of symmetry of the model is far away from the wind tunnel centerline because of the shape of the model. The blockage is as high as 24 % which is quite significant and would influence significantly on the pressure results. Because of this reason the model CL was introduced to lower the height and the blockage ratio. However, as in the model BL, the building height and the parapet ratio are not simulated .

  These distortions of the building height, the parapet ratio and the blockage ratio will be analyzed in a later chapter where additional tests were conducted for this purpose.

3.4 Instrumentation

The model was always placed in a 45° diagonal direction against wind (Figs. 3.4-3.11) since this orientation represents the most critical situation that gives the worst roof suction amplified by the vortices as mentioned.

The upwind triangular corner ($17cm \times 17cm \times 24cm$) of the model is made of plexiglass and has been instrumented by 92 pressure taps as shown in Fig. 3.12, connected to Sytra differential pressure transducers through Scanivalve switches. The tubes connecting pressure taps to the transducers are about 18cm long which is short enough to avoid any complexity in distortion of pressure signals due to acoustic resonance characteristics though the pressure results discussed in this thesis are all mean values anyway. The sampling rate was 250 Hz for a period of 15 s for each run at the reference wind speed of 5.0m/s at the building height. For each pressure tap, both the mean and the root mean square pressure coefficients plus the minimum and maximum values occurring for each measurement were recorded. Examples of tabulated data is shown in Appendix A

3.5 Data Analysis

For comparison of flow patterns, contour lines (Appendix C) of mean dimensionless pressure coefficients are used.

Pressure coefficient C_p is defined as the ratio of the mean dynamic pressure at the measured point $(P - P_0)$ to the mean dynamic velocity pressure $\frac{1}{2}\rho V^2$:

$$C_p = \frac{P - P_0}{\frac{1}{2}\rho V^2} \tag{3.3}$$

where

P = the mean local pressure at the tapping point.

P_0 = the static reference pressure.

V = the mean velocity at the roof height.

ρ = the density of air.

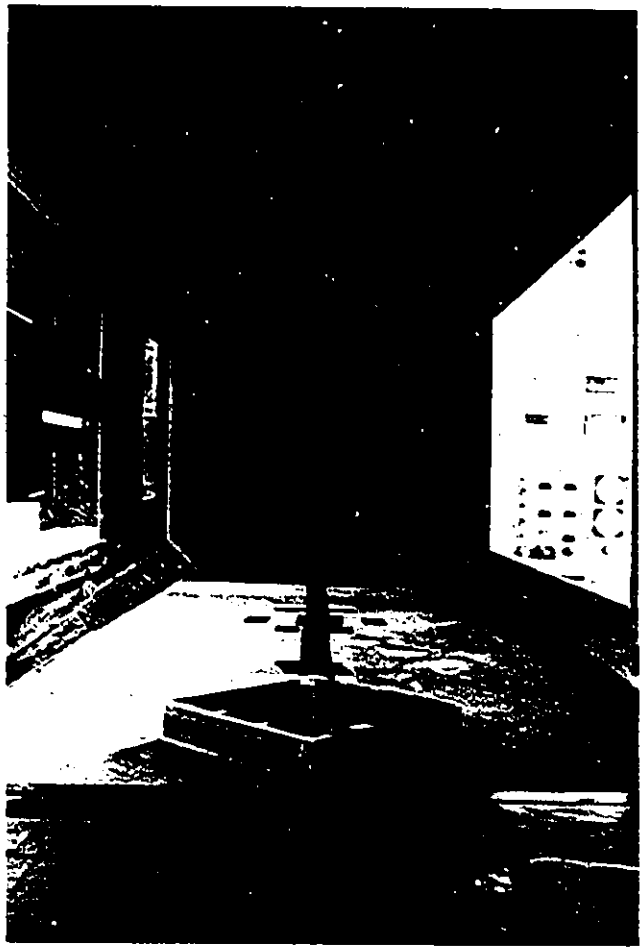

Figure 3.4: Model ALW

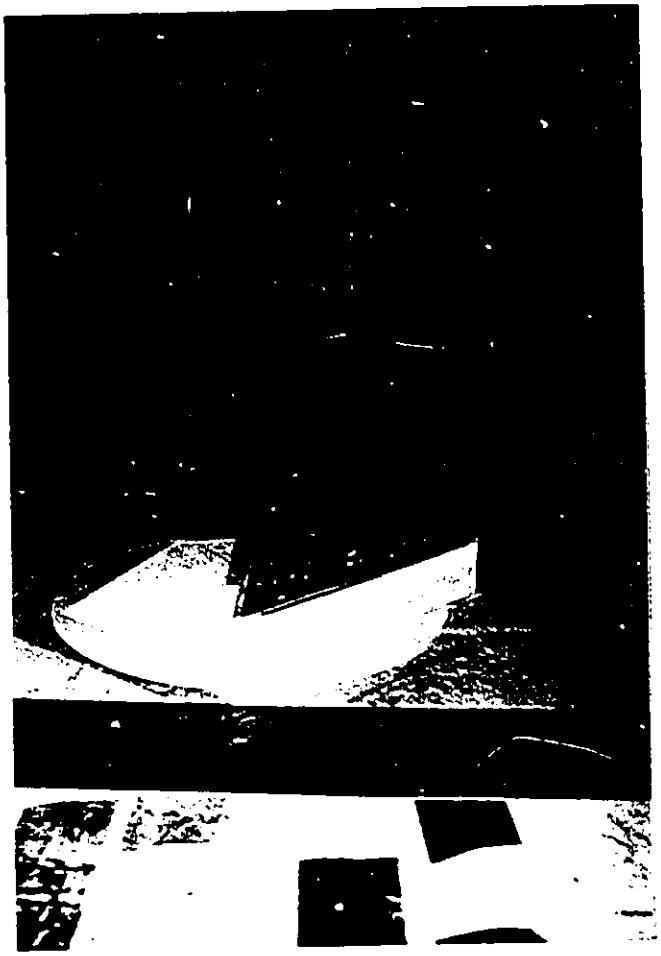

Figure 3.5: Model ALH

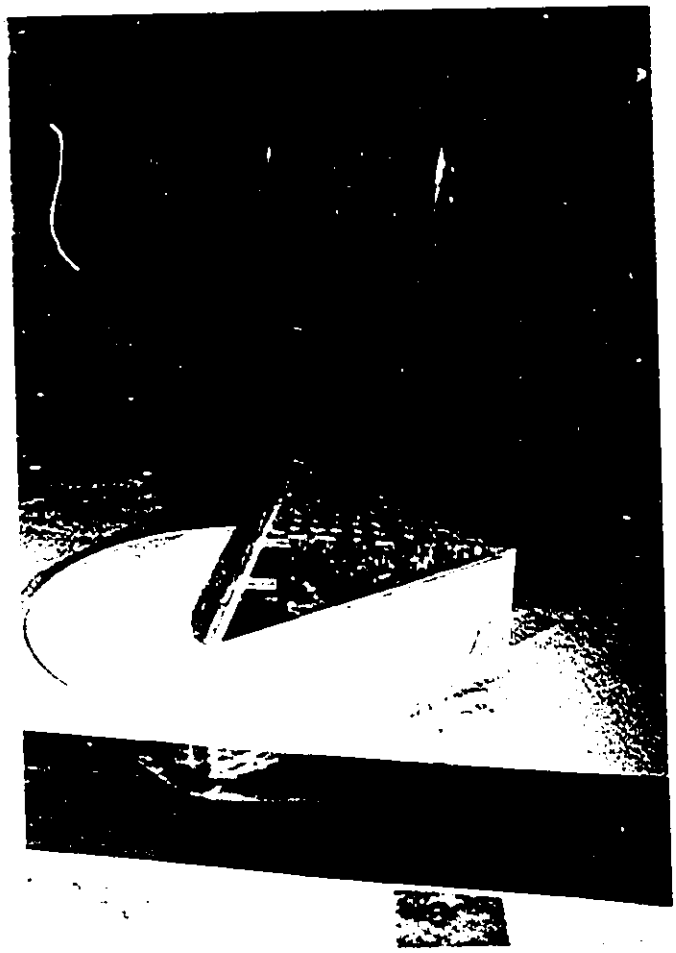

Figure 3.6: Model ALHP

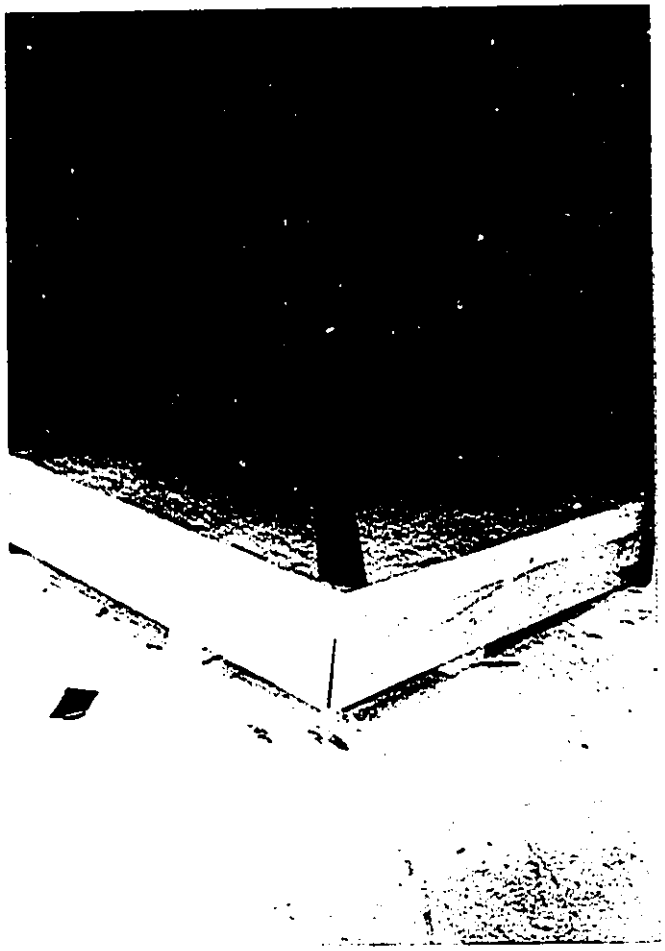

Figure 3.7: Model BHW

Figure 3.8: Model BLW

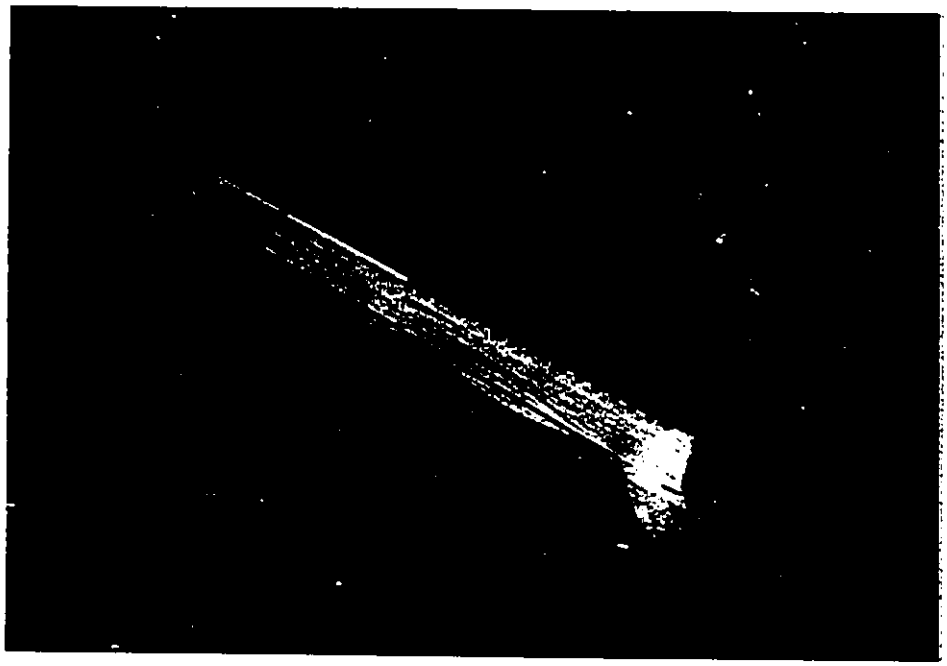

Figure 3.9: Model BLHPL

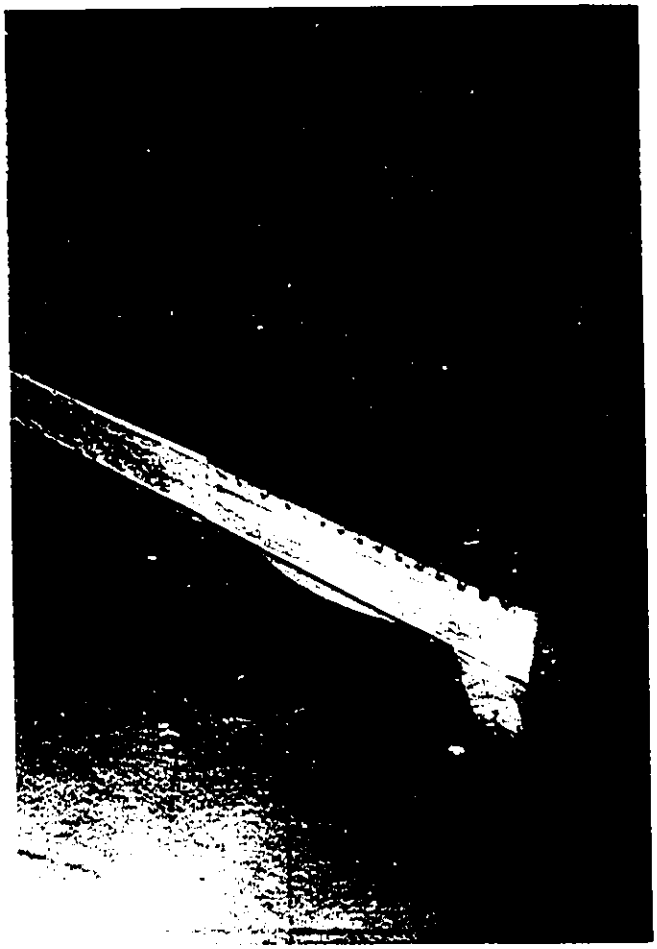

Figure 3.10: Model BLHPH

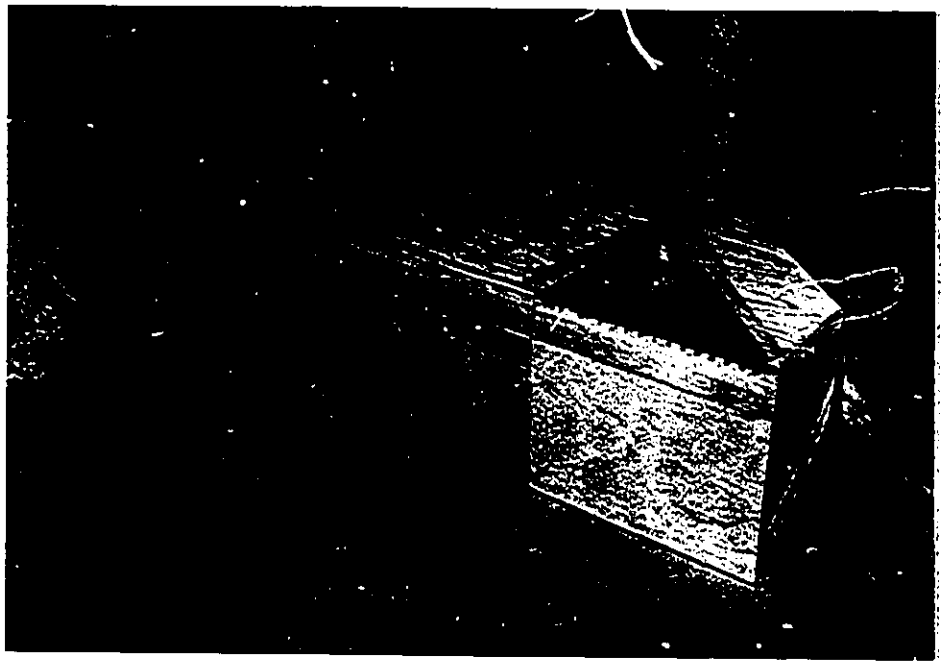

Figure 3.11: Model CH

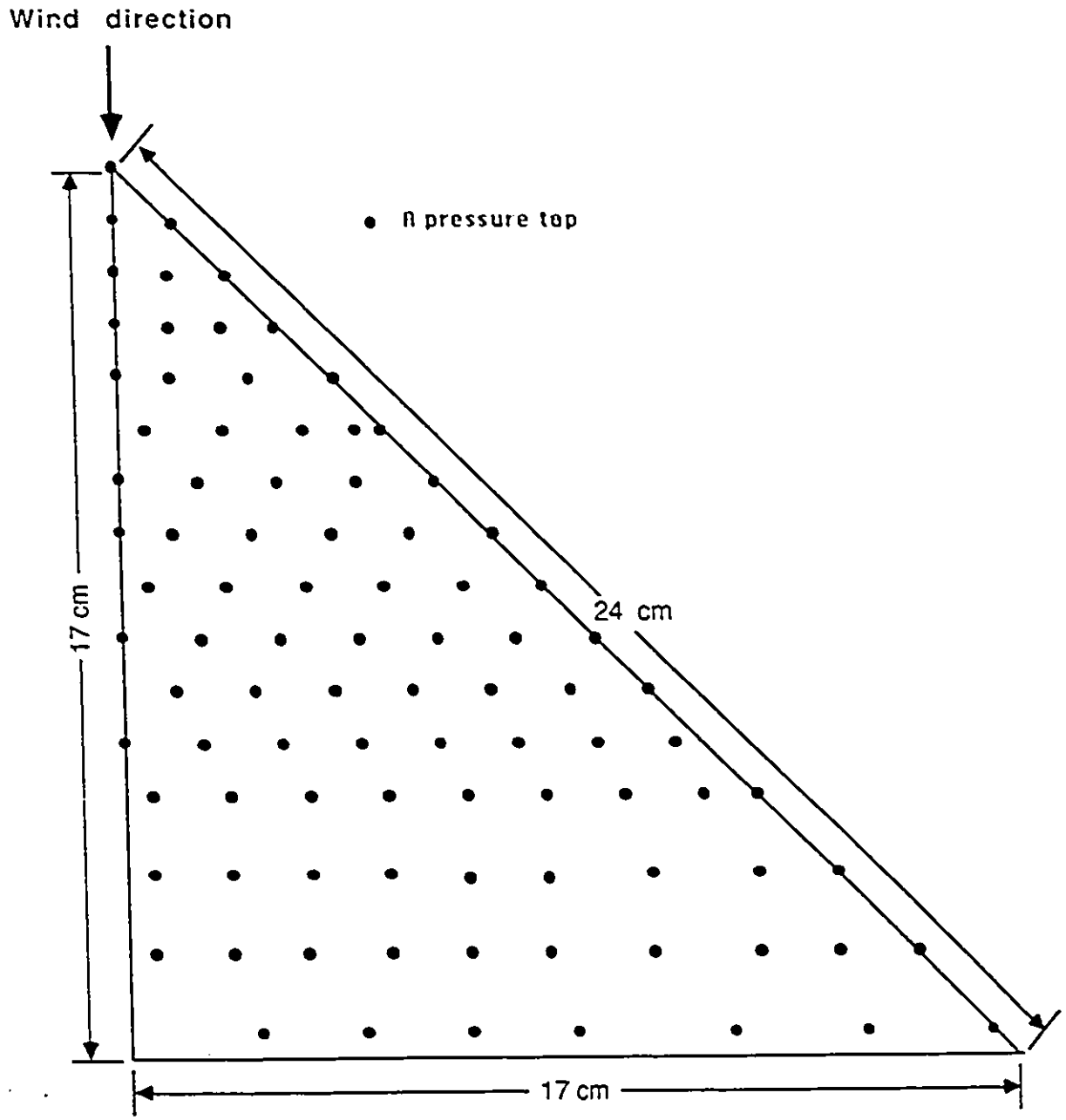

Figure 3.12: Distribution of Pressure Taps

Chapter 4

Experimental Results and Discussion

4.1 Comparison with Previous Studies

The pressure distribution on smooth roof areas depends mainly on the flow field around the building and on the characteristics of the oncoming flow. Important building parameters influencing the pressure distributions are the side length/width ratio (L/B), height/width ratio (h/B), the wind yaw angle and the relative parapet height (h_p/B) [23]. In other words, the building shape, wind direction and parapet height are the major parameters. If these three parameters are kept constant, the distribution of dimensionless pressure coefficients are expected to be more or less invariant [11].

An important question, therefore, is whether or not the test results from

the model ALW (1/100 model) are comparable to the previous 1/10 model test results [3] regardless the difference in Reynolds number and the turbulence used in the tests.

Fig. 4.1 shows the wind induced pressure contours over the critical region of the roof deck obtained from 1/100 and 1/10 scaled models. This direct comparison shows the repeatability of the flow pattern over the high suction area and even the values of coefficients under different scaling factors are quite similar as expected.

Overall, the present test results show a good agreement with the previous ones and can be considered to be reliable as a pilot study for the future tests at the 9m × 9m wind tunnel.

4.2 Effect of Linear Scale

Through the present series of wind tunnel tests, the same instrumented portion of the model was used even when the size of the model was different. It means that different proportions with respect to the model size were instrumented for pressure measurement. This has to be taken into account when comparing two test results in different linear scales. Figs. 4.2 and 4.3 present the results of three different models; ALW(scale 1/100), BHW(scale 1/37.5) and CH(scale 1/21). Fig. 4.2 is a superposition of the results from ALW and BHW. Fig. 4.3 is a superposition of all three sets of results having the scaling

factors adjusted to be compared to the results of the model BHW.

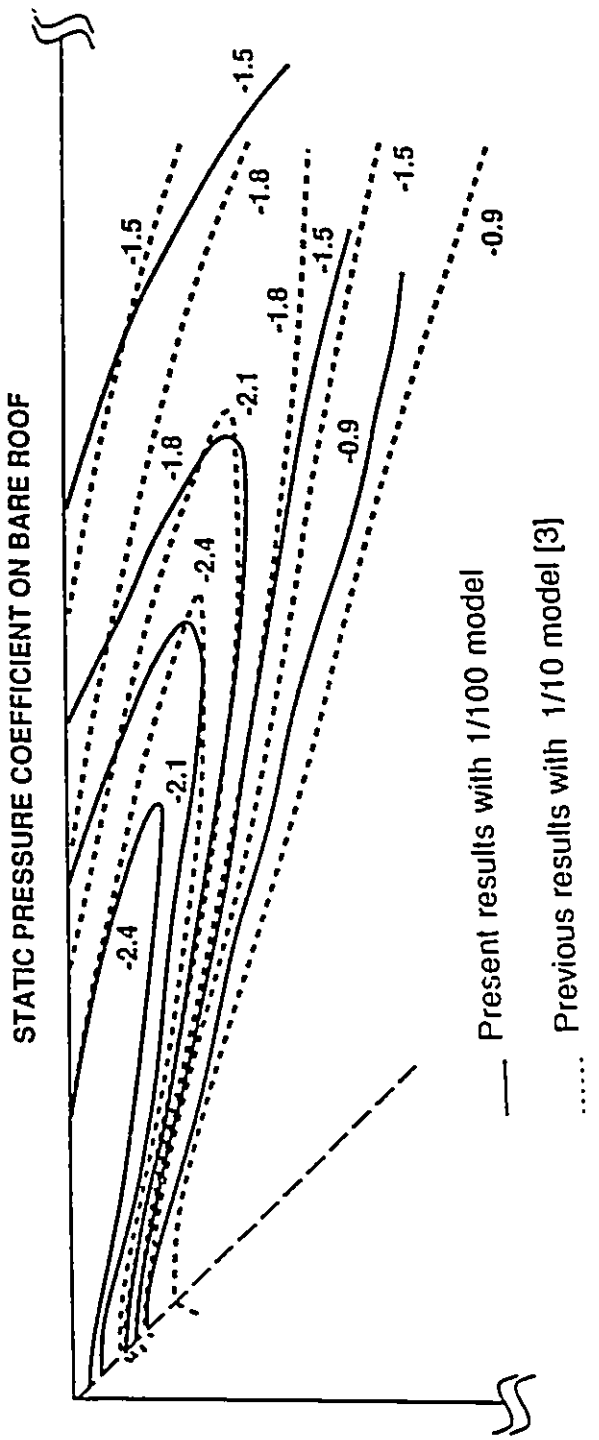

Figure 4.1: Comparison of the Present Results with Previous Test Results

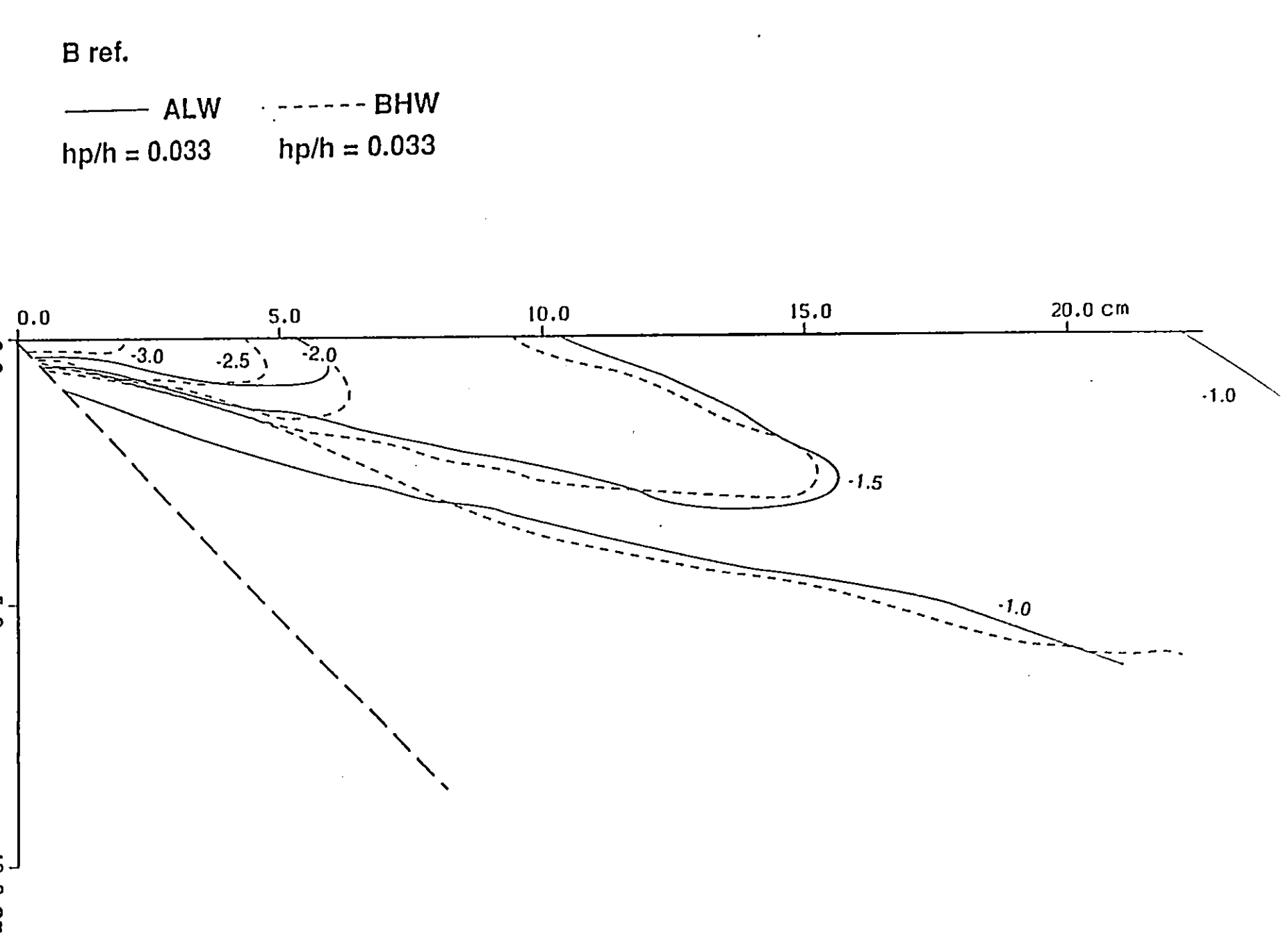

Figure 4.2: Mean pressure coefficients :ALW and BHW

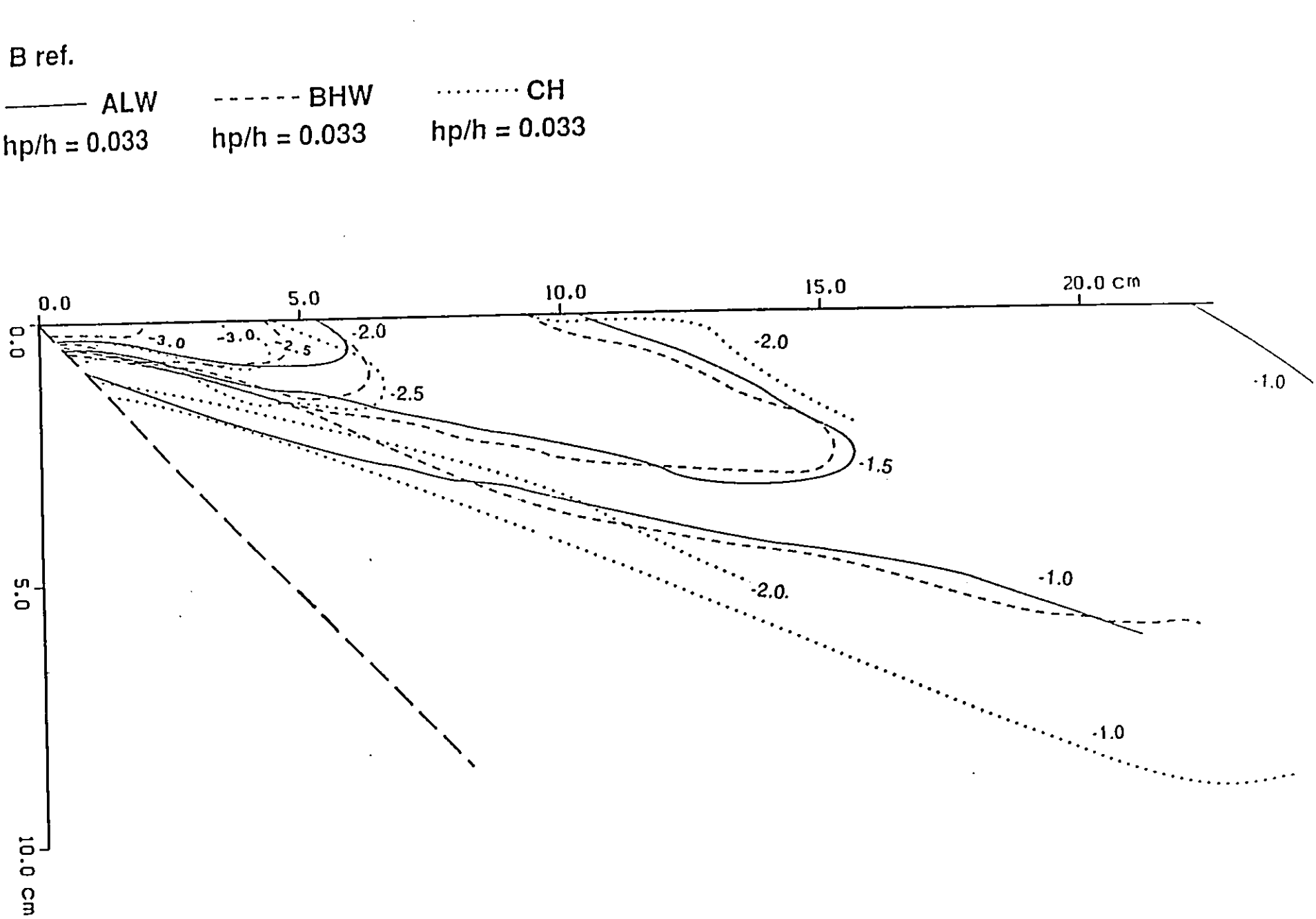

Figure 4.3: Mean pressure coefficients :ALW, BHW and CH

The results from ALW and BHW are very similar both qualitatively and quantitatively. It should be noted that the important parameters, wind direction, building configuration and parapet ratio are kept identical for these two cases. This observation confirms the statement made at the beginning of this chapter regarding three major parameters. However, the model CH which also has these three parameters identical gives much higher suction coefficients. This is obviously caused by an accelerated air flow due to high wind tunnel blockage ratio (24%).

In terms of the aerodynamic simulation, the wind tunnel blockage is no doubt a deficiency. However, even if the aerodynamic similitude requirements are not properly satisfied with this model, this particular case has an interesting application for engineering purposes. As it was briefly mentioned in Chapt.1, one of the original purposes of this series of wind tunnel tests was to examine the effectiveness of structural details of roof structures against wind induced high suction on flat roofs. Although the induced suction by wind on the model CH is not a good simulation of the original case, as long as the suction pattern is more or less similar to the expected one, the high wind tunnel blockage can be even utilized to obtain the same pattern of pressure coefficients with exaggerated magnitude of suction. This model CH is then a reliable tool even though pressure magnitude is exaggerated. More attention will be paid to the model CH in the next chapter where the blockage effect will be discussed in more detail.

The test results show that the difference of a linear scaling factor would not change the characteristics of the vortex induced high roof suction and any linear scale is adequate to give the required information as long as other significant factors are properly taken care of. This result is consistent with the previous comparison in section 4.1.

4.3 Comparison of Full/Half Models

4.3.1 Concept of Symmetry

Pressure distribution on the roof of the building due to wind action is dependent on wind direction relative to the building. When the yaw angle is chosen to be 45°, since this is found to be the most critical case, both sides of the diagonal division line of the roof are under the same wind loading pattern because of the symmetry. The vortices are generated along both edges of the roof in the same manner because of the symmetry of the structure and of the air flow characteristics about the wind tunnel centerline. This was illustrated by many experimental results where different building shapes and sizes with various parapet heights were tested [24].

4.3.2 Testing of Half Models

The testing of half models is to examine this concept. Fig. 4.4 shows the results from ALW, ALH (the half model of ALW) and ALHP (ALH with a vertical split plate). As it is obvious no significant difference is observed between the results of ALH and ALW. The repeatability of the results of ALW by ALH is in fact quite good. A slight increase in suction can be observed. This deviation can be estimated by calculating the area covered by each contour line. When the area is reduced that means an increase in suction.

For $C_p = -2$ and $C_p = -1.5$ the area is reduced to about half of the area covered by the same contour lines in ALW. For $C_p = -1.0$ the area is reduced by about 25%. This deviation was probably caused by the change of flow characteristics due to the loss of structural symmetry.

For the improvement of the similarity with the half model, a thin vertical split plate along the line of symmetry was placed in order to possibly enhance the two dimensionality of the model/flow interaction. The model ALHP, the half model of ALW with the split plate, is shown in Appendix B. The results of this model are summarized in Appendix C. From Fig. 4.4 also; the results from the model ALHP are improved. This can be observed by the fact that the contour lines are closer to those of ALW but there is still a smaller deviation estimated by an increase in suction by 25% for $C_p = -2.0$ and about 15% for $C_p = -1.5 and - 1.0$

Similar results are illustrated in Fig. 4.5 with models in larger scale: BLW, BLHPL and BLHPH. BLHPL and BLHPH are very similar half models of BLW except two different heights of split plates are used; a lower plate in BLHPL and a higher plate in BLHPH. The purpose was to examine how long and how high should the plate be to give better simulation of the whole model case. In BLHPL the plate is of the same height as the roof parapet whereas in BLHPH the plate is about the building height higher than the building itself. Both plates are sticking out of the windward corner of the model and have sharp front edges to avoid aerodynamic interference.

As it is seen in Fig. 4.5, the results from BLHPL and BLHPH are not significantly different but a little better agreement with the whole model, BLW, seems to be given with the higher plate (BLHPH). Two cases would not be really enough to decide a definite size of the most efficient plate.

What was proved here is that the results from half models show a good agreement with the whole model results. Hence, the prediction of the high suction on a flat roof of a building can be made from the test results of a half model or possibly even of a smaller portion of the half model configuration where the high suction is expected to occur, namely the upwind corner of the roof.

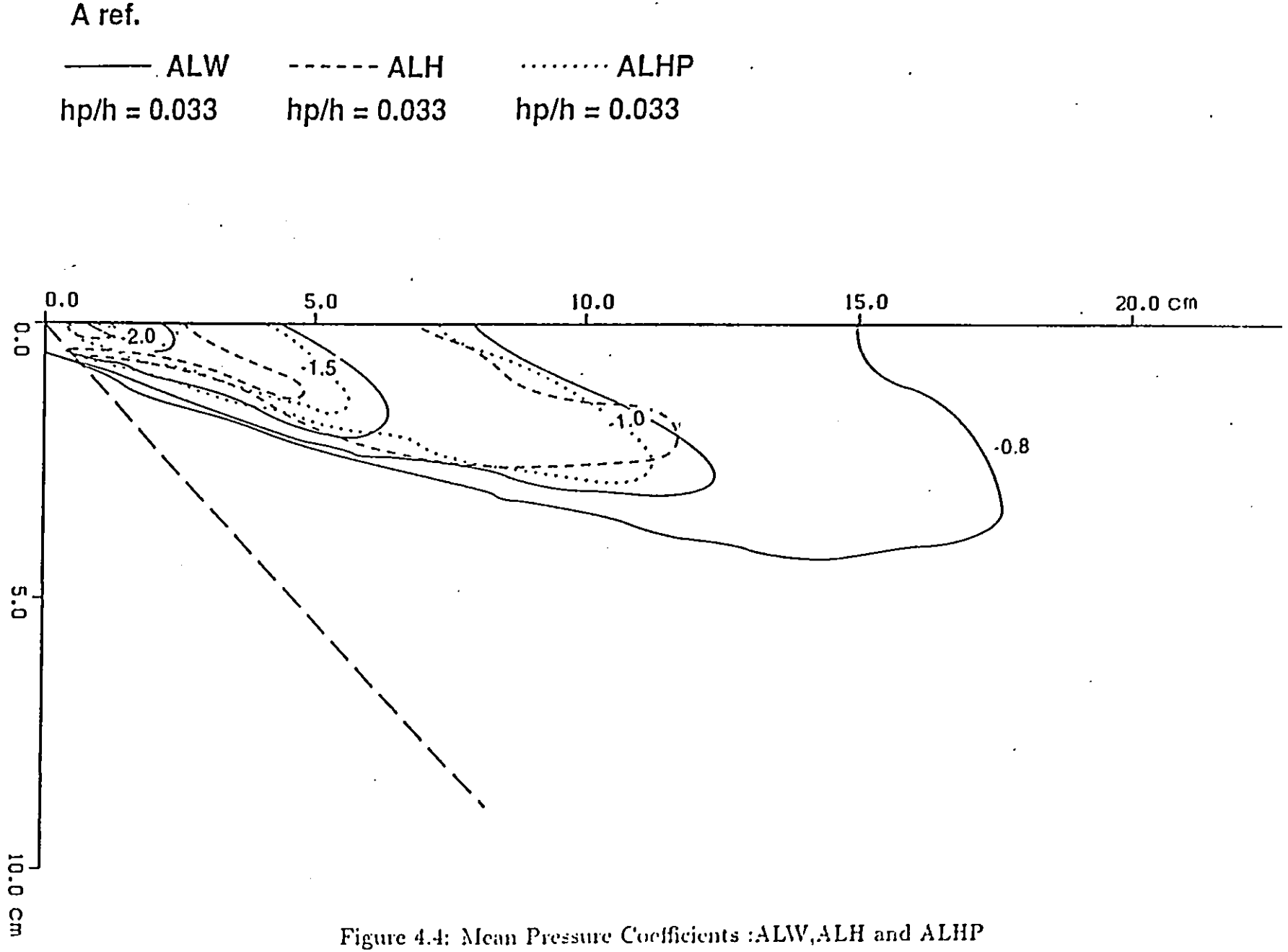

Figure 4.4: Mean Pressure Coefficients :ALW,ALH and ALHP

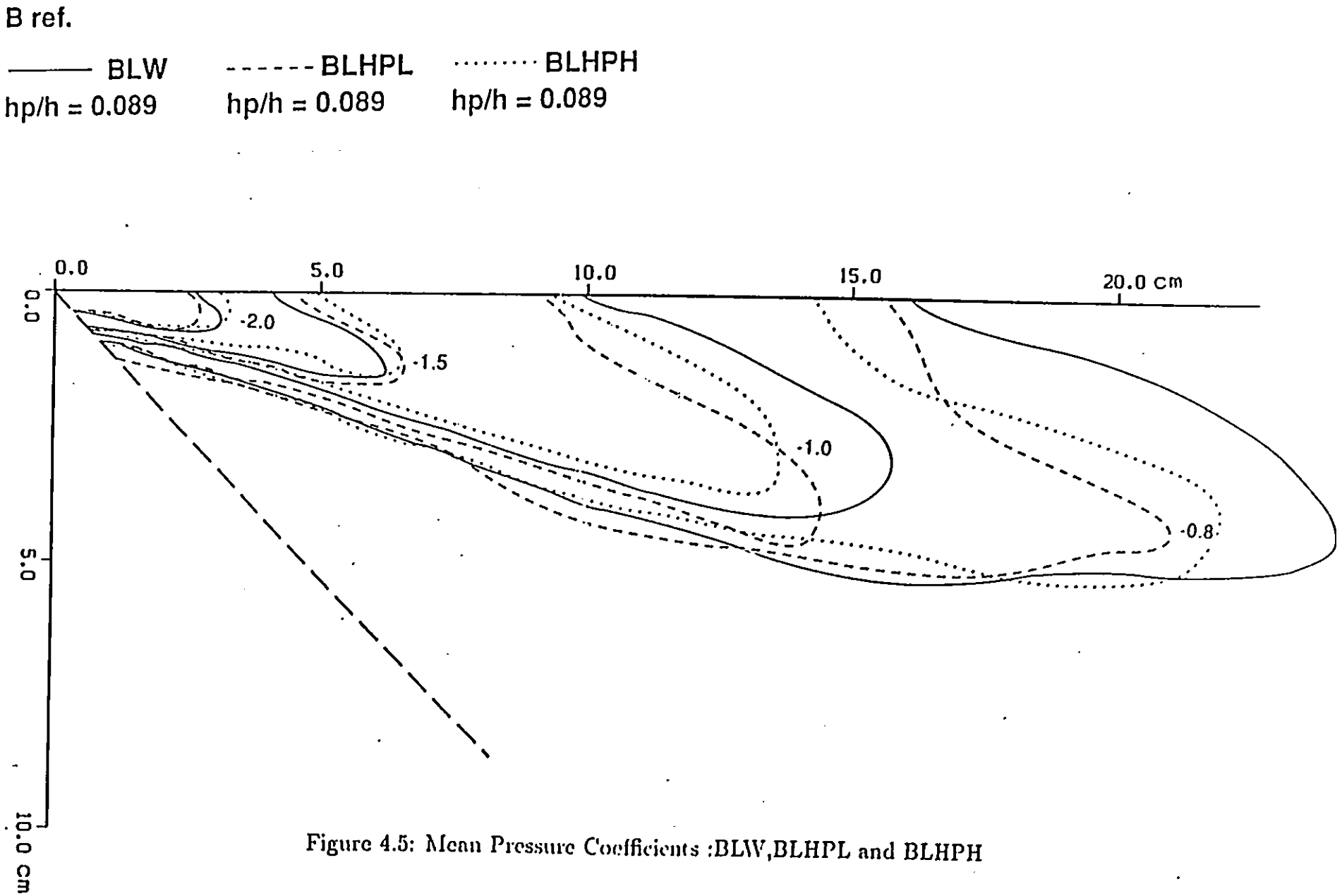

Figure 4.5: Mean Pressure Coefficients :BLW,BLHPL and BLHPH

4.4 Pressure Distribution over Larger Area

The large model CH is the model that did not give good agreement with ALW and BHW, though the model had the same major parameters: wind direction, parapet ratio h_p/h and building configuration. However, there was one obscurity in the comparison, which is the fact that a relatively small portion of the model was instrumented with pressure taps and therefore when the adjustment due scaling factor is needed this model covered a smaller portion of the roof to be compared with others.

In order to improve this deficiency, an additional set of tests was performed with wider distribution of pressure taps over the whole roof of the model. The comparison with ALW can then be done directly.

Fig. 4.6 shows the results from the model CH with larger area tested. If Fig. 4.6 of CH and Fig. C. 1 (Appendix C) of ALW are superimposed some deviation is still present which can be most likely attributed to the blockage effect since the blockage ratio is quite high. This point is again discussed in the next chapter.

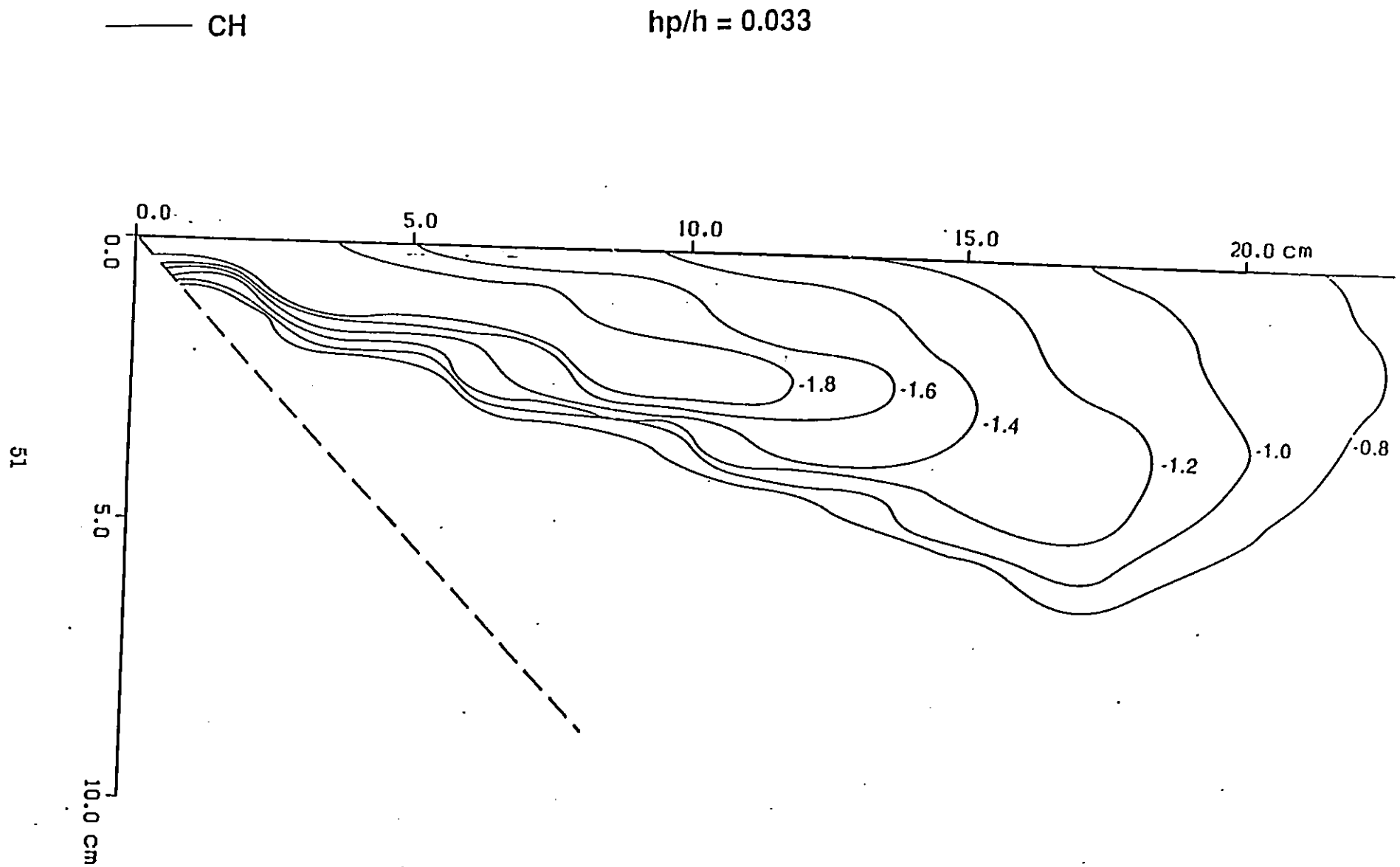

Figure 4.6: Mean Pressure Coefficients: model CH

Chapter 5

Effects of Other Parameters on Pressure Distribution

5.1 General

In any parametric analysis, if the effect of one particular parameter is to be examined precisely, all other parameters need to be kept invariant. Otherwise, the joint effects of more than one parameter can be reflected on the results and one cannot identify the effect of each parameter separately.

In fact in Chapt.4, some of the parameters were modified simultaneously with other parameters. For example, the change of the building height without changing the parapet height will modify, of course, the parapet height ratio and both parameters, the parapet ratio and the building aspect ratio, would probably influence on the test results.

In order to further study this point, an additional set of tests was conducted in the same wind tunnel with almost the same characteristics. Several models tested are described in the next sections and the results of the new experiment are believed to be as reliable as the previous ones. Fig. 5.1 shows the repeatability of the mean pressure coefficient of the same model ALW measured 4 months apart. The agreement between them seems to be reasonably good.

5.2 Effect of Parapets

One of the very common features of flat-roofed buildings is the existence of parapets, which are low walls around the edges of the roof.

Parapets are usually integral parts of the external walls of the building and are designed to provide positive anchorage of the roof to the structure [25]. However, parapet may also be beneficial in reducing local extreme wind suction by more or less equalizing the wind pressure distribution over the roof surface [26].

Since the occurrence of extreme suction often causes wind induced damages to the cladding and roofing system, parapets represent an architectural feature as well as a safeguard against wind.

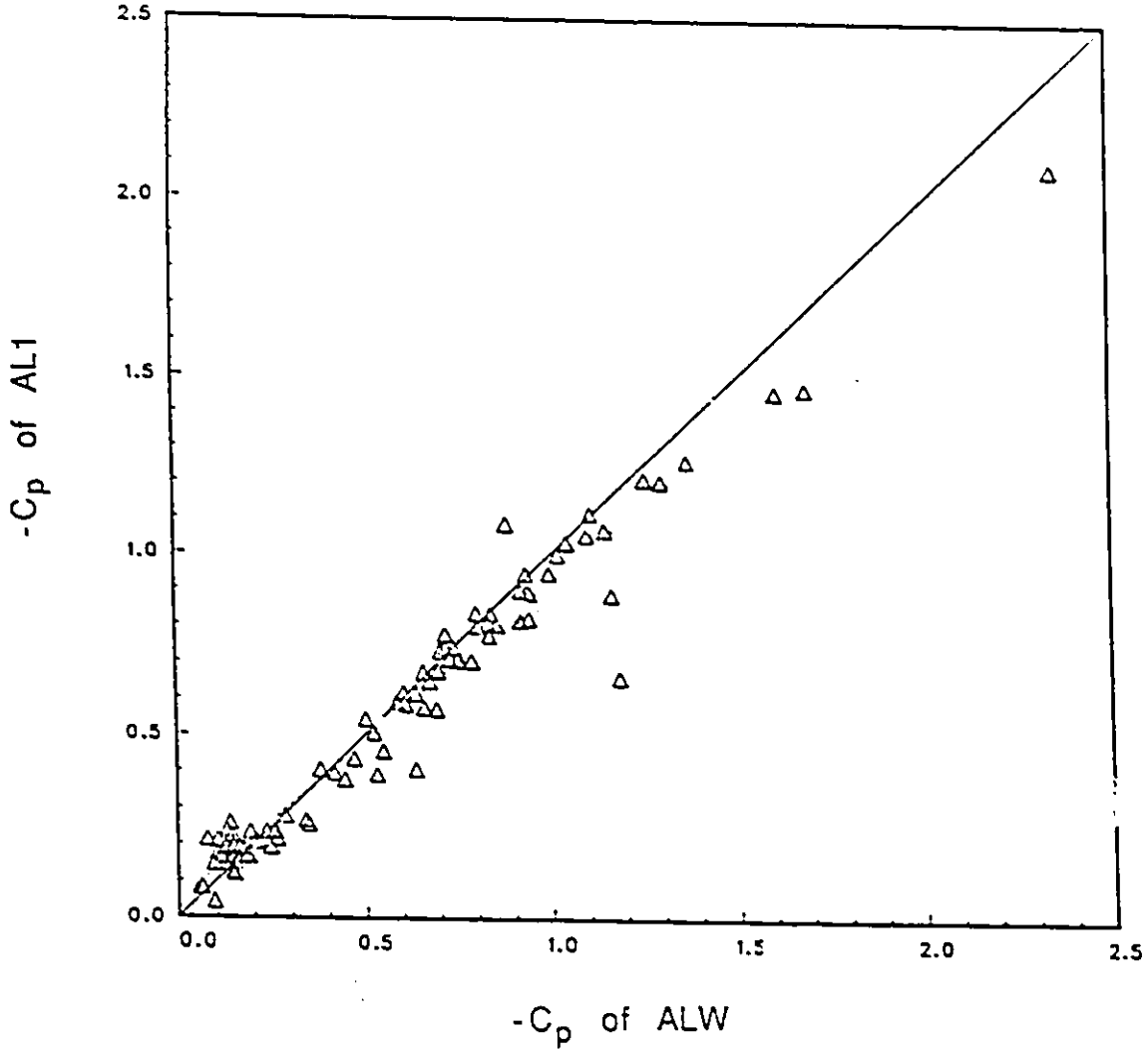

Figure 5.1: Repeatability of C_p of ALW in AL1 tested 4 months later

5.2.1 Previous Research Results

As we observed through literature review in Chapt.2, the previous research on parapet effects on pressure has shown that the use of parapets would cause the following:

- A drastic reduction of suction at the corners and edges.
- A reduction of suction in uniform flow but no reduction on mean pressure coefficients in turbulent flow.
- Increase in suction with low parapet.
- A significant change only in the corner pressure coefficient.
- Increase of roof corners mean pressure coefficient.
- A reduction of peak pressure coefficients.
- Reduction of both mean and peak suction.
- A reduction on edges but an increase of suction on corners.
- A reduction of peak pressure in the edge.
- An increase of mean pressure in edges.
- Increase of both mean and peak suction at corner region.
- A slight increase of suction on interior areas.

These statements, as mentioned before, are obviously somewhat contradicting each other. It can be at least partly attributed to the interaction with other parameters.

5.2.2 Present Results

In order to examine the parapet effects on wind induced pressure more specifically, the small model previously defined as ALW was chosen as the basic model so that the results are not contaminated by the wind tunnel blockage effect. The blockage for this case is less than 5 %.

The model ALW was modified with different parapet heights while all other parameters were kept invariant. These modified models are summarized in Table 5.1. AL1 is the same as ALW itself. In addition, both AMW and AHW without parapets were tested, these are listed in Table 5.1 as AM0 and AH0.

Fig. 5.2 gives $-C_p$ of AL0, AM0 and AH0 together with ALW, AMW and AHW to show the overall effect of parapets. With the exception of corner areas, the overall effect of parapets is found to be a reduction of the wind loading, which confirms previous results of refs. 19 and 20. In all three plots in Fig. 5.2 of three different models ALW, AMW and AHW the majority of the points are slightly under the diagonal line of slope 1/1 with the exception of some points which are located at the corner.

Nevertheless, the influence of the building height on the effect of a parapet

is also clear. More reduction in the magnitude of pressure coefficient has been observed for taller buildings(AMW and AM0, AHW and AH0) rather than for lower buildings(ALW and AL0). The effectiveness of the parapet height is hence related to the building height [6]. When the dimensionless ratio of the parapet height to building height h_p/h is used as a parameter, as it was previously discussed in literature review, we do not have this problem.

Fig. 5.3 illustrates the pattern of wind induced suction by the equi-pressure contour lines of the models AL0, AL1, AL2, AL3 and AL4.

When the parapet height ratio was increased from zero in AL0 to 0.033 in AL1 and then to 0.067 in AL2, the area surrounded by each contour line for a given suction coefficient becomes smaller which means a reduction in total suction. However S3 and S4 show an increase in suction when h_p/h is increased. The rate of change of the area under each contour line against the change of h_p/h is not constant. A plot of $-C_p$ against the area covered by each contour line of a specific $-C_p$ is shown in Fig. 5.4.

In Fig. 5.4, if the cross-section of these curves at the same $-C_p$ value is taken, the decrease and then increase of area corresponding to a given $-C_p$ are observed here again with the increase of h_p/h.

Table 5.1: Models tested for parapet effect

Model No.	Building height h (cm)	Parapet height h_p (cm)	Parapet ratio h_p/h
AL0	4.50	0.00	.000
AL1	4.50	0.15	.033
AL2	4.50	0.30	.067
AL3	4.50	0.45	.100
AL4	4.50	0.60	.133
AM0	9.00	0.00	.000
AH0	12.00	0.00	.000

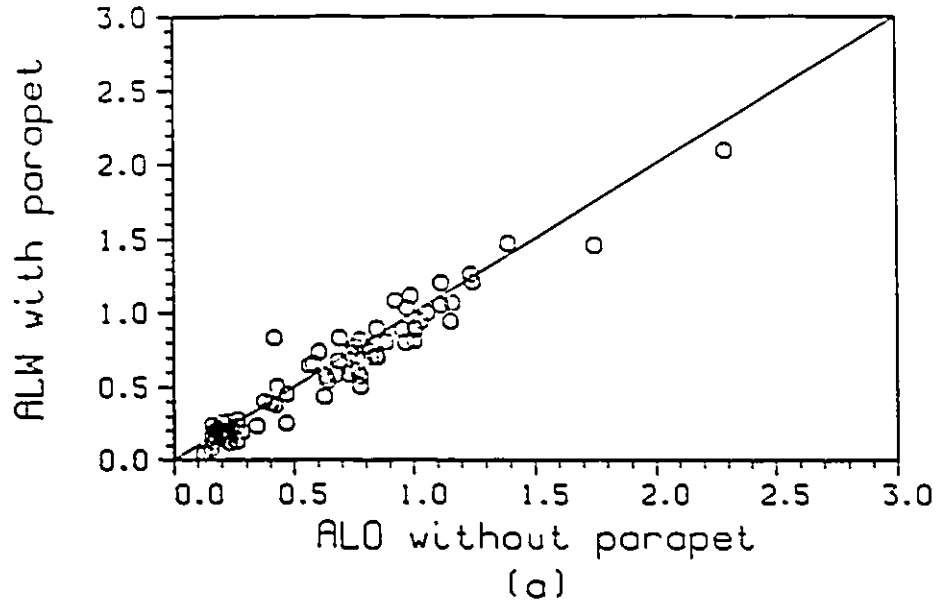

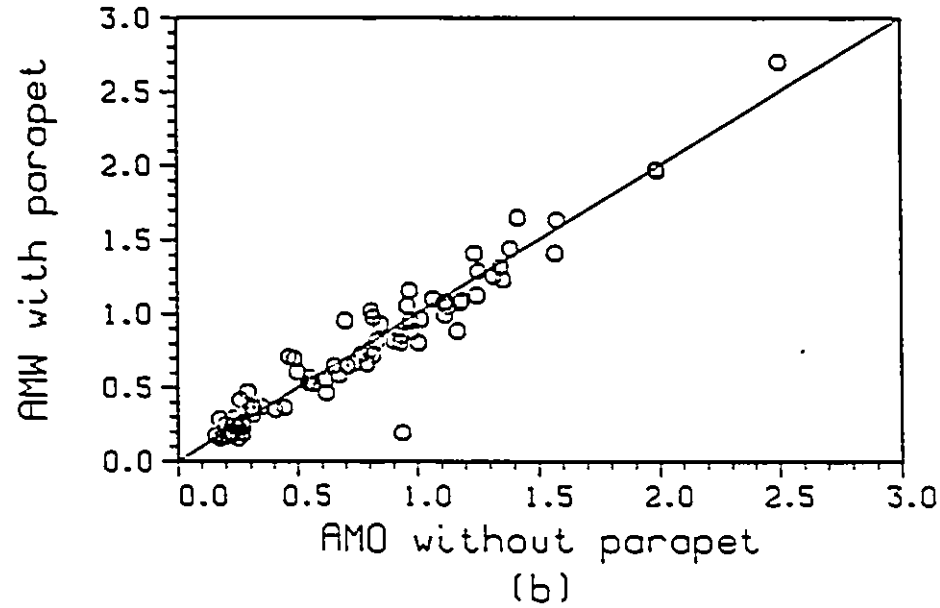

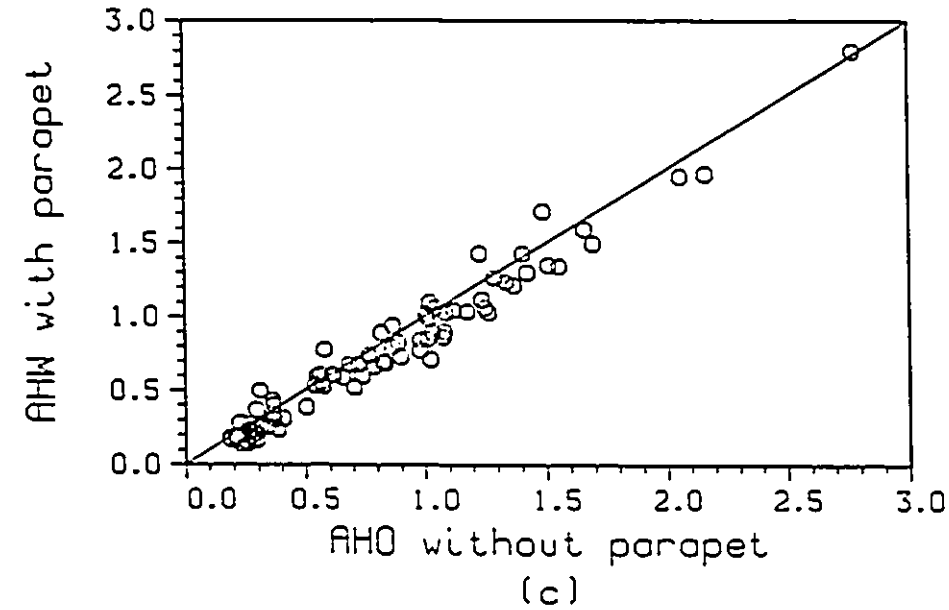

Figure 5.2: Overall Effect of Parapet

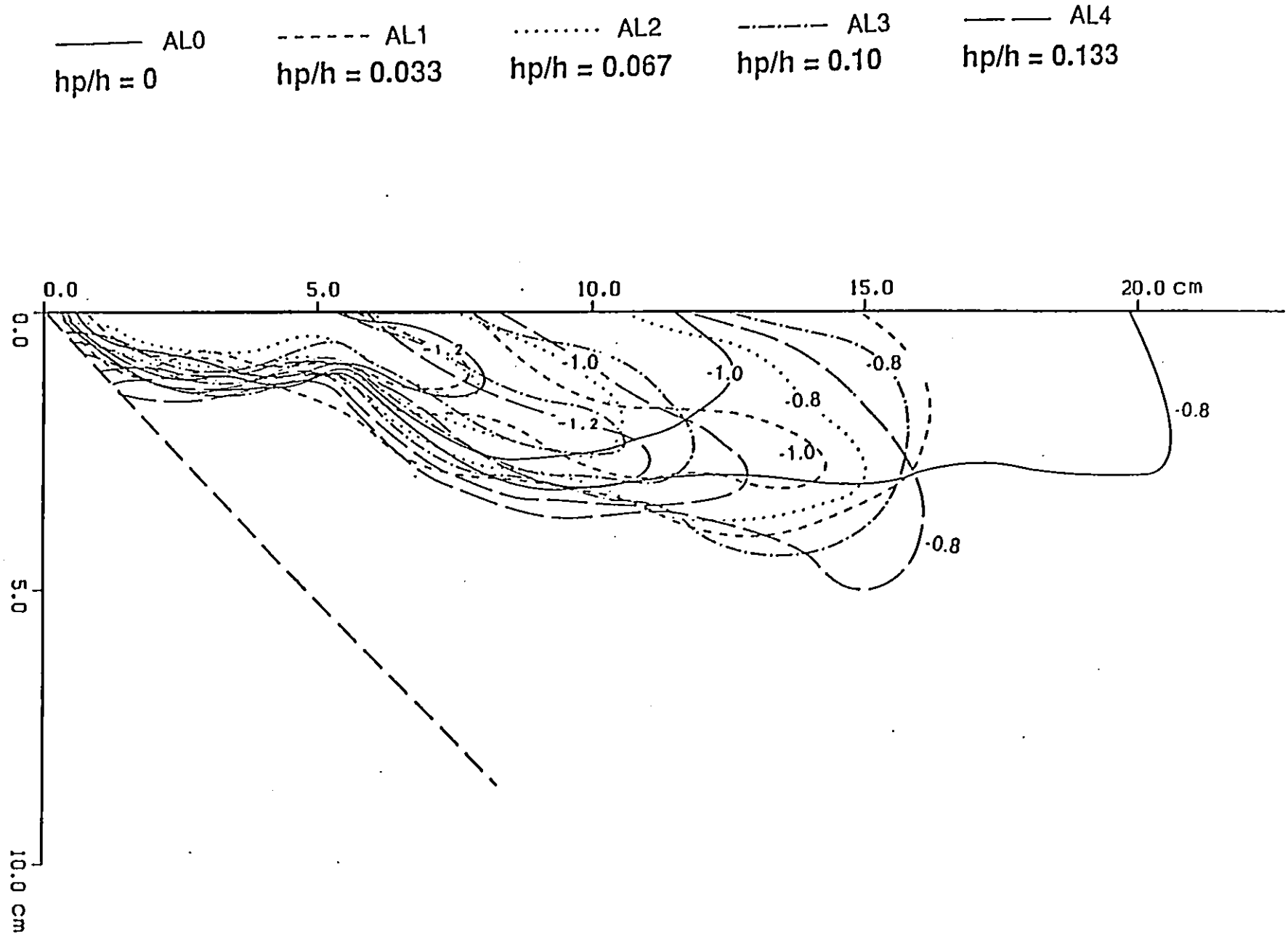

Figure 5.3: Mean Pressure Coefficients on Models with different Parapet ratios

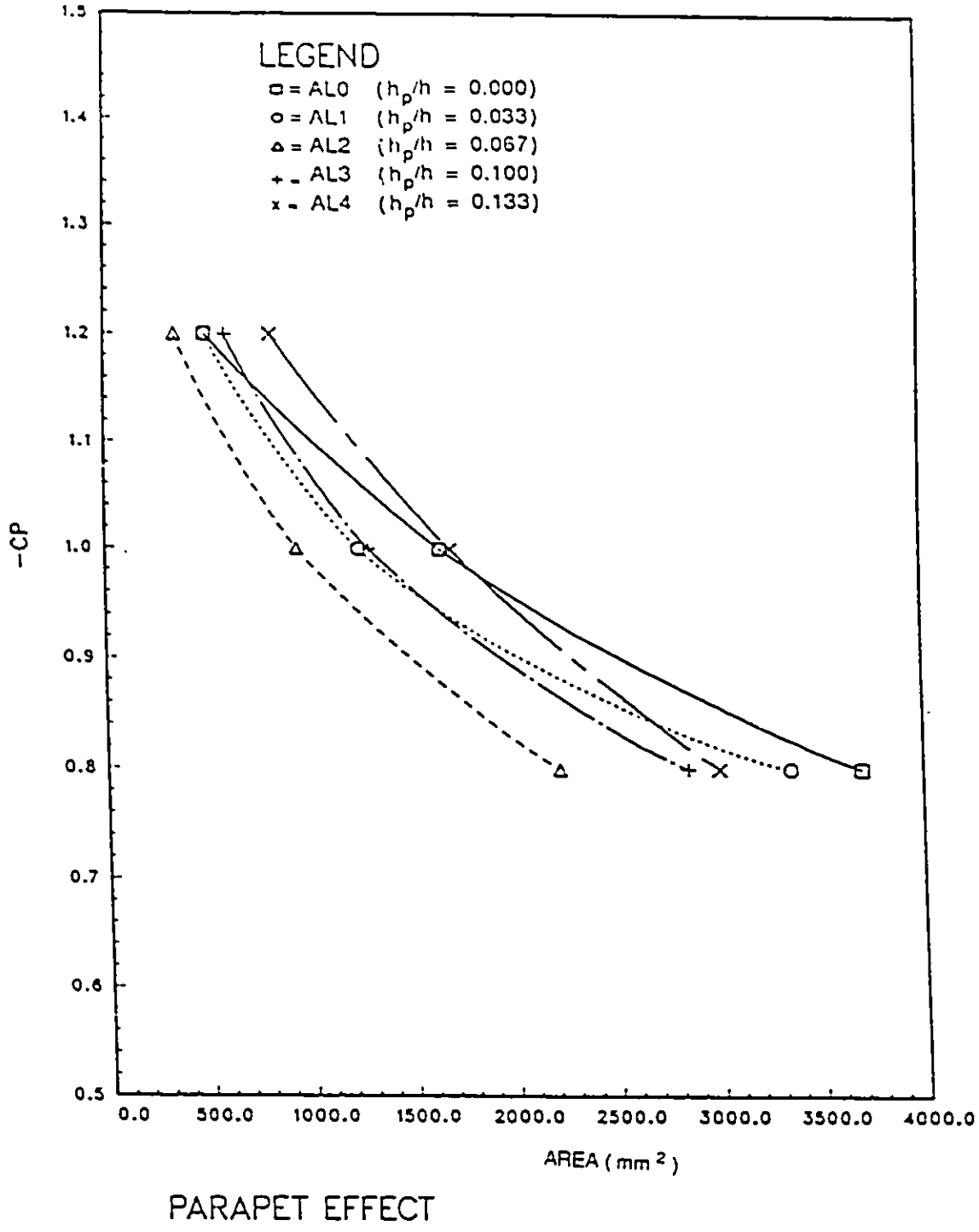

Figure 5.4: Parapet Effect on Mean Pressure Coefficient

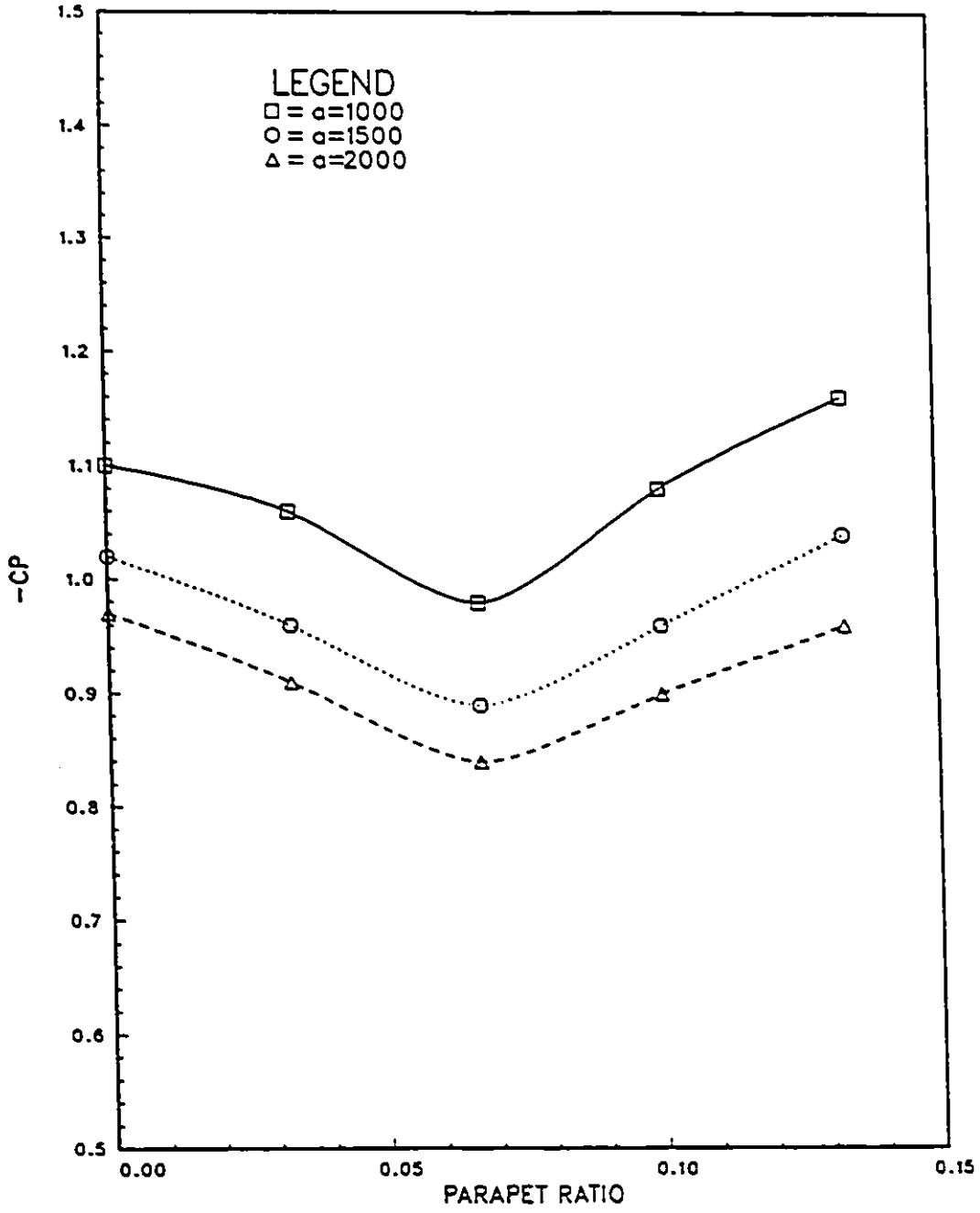

Figure 5.5: Parapet Effect on Mean Pressure Coefficient

This observation is better explained in Fig. 5.5 which is derived from Fig. 5.4 and presents the results of $-C_p$ against parapet ratio h_p/h for three different areas. Fig. 5.5 can be used for the prediction of C_p for any given parapet ratio in this range.

It can be concluded from this section that the effect of parapet on wind induced suction on flat roofs depends on the parapet height ratio. It can reduce the magnitude of suction when the parapet ratio is less than a certain value, 0.07 for this case. However, the magnitude of roof suction increases if the parapet ratio is higher than this value. This reverse of tendency is because if the parapets are too high a creation of stronger vortices is probable and therefore higher suction is registered.

5.3 Effects of the Building Height

The small model ALW, was again chosen to further examine the effects of the model building height in this section so that no blockage effect would be involved. Even with the tallest model, the blockage ratio was less than 5%.

Three models with different model heights keeping the parapet ratio constant were used as shown in Table 5.2. The model ALh1 is the same model as ALW

When ALh1 is compared with ALh2 in Fig. 5.6, the increase of suction is

observed i.e the area under each equi-pressure contour line is greater for ALh2. The same tendency is observed between ALh2 and ALh3, namely the increase of the building height gives increase of the suction. This can be explained by the fact that when the building is higher, the case considered as a building with less exaggerated scale and only a portion of the building is tested. Therefore the graph of this case should be compared to the corresponding portion of the other cases. For example, using a medium height ALh2 as the reference, the shorter model ALh1 should be enlarged and the taller model ALh3 should be scaled down to the corresponding portion.

Figs. 5.7 and 5.8 present the same results more quantitatively. For a specific parapet ratio of 0.033, in Fig. 5.7 the C_p is plotted against the area under each contour line for three different heights of the building. Fig. 5.8 is derived from Fig. 5.7 presenting the results as C_p plotted against the building height for three different areas. The conclusion is that the increase in building height leads to higher suction. The change of C_p as a function of building height can easily be computed for a specific parapet height

Table 5.2: Models tested for the height effect

Model	Building height h (cm)	Parapet height h_p(mm)	Parapet ratio h_p/h
ALh1	4.50	0.15	.033
ALh2	9.00	0.30	.033
ALh3	12.00	0.40	.033

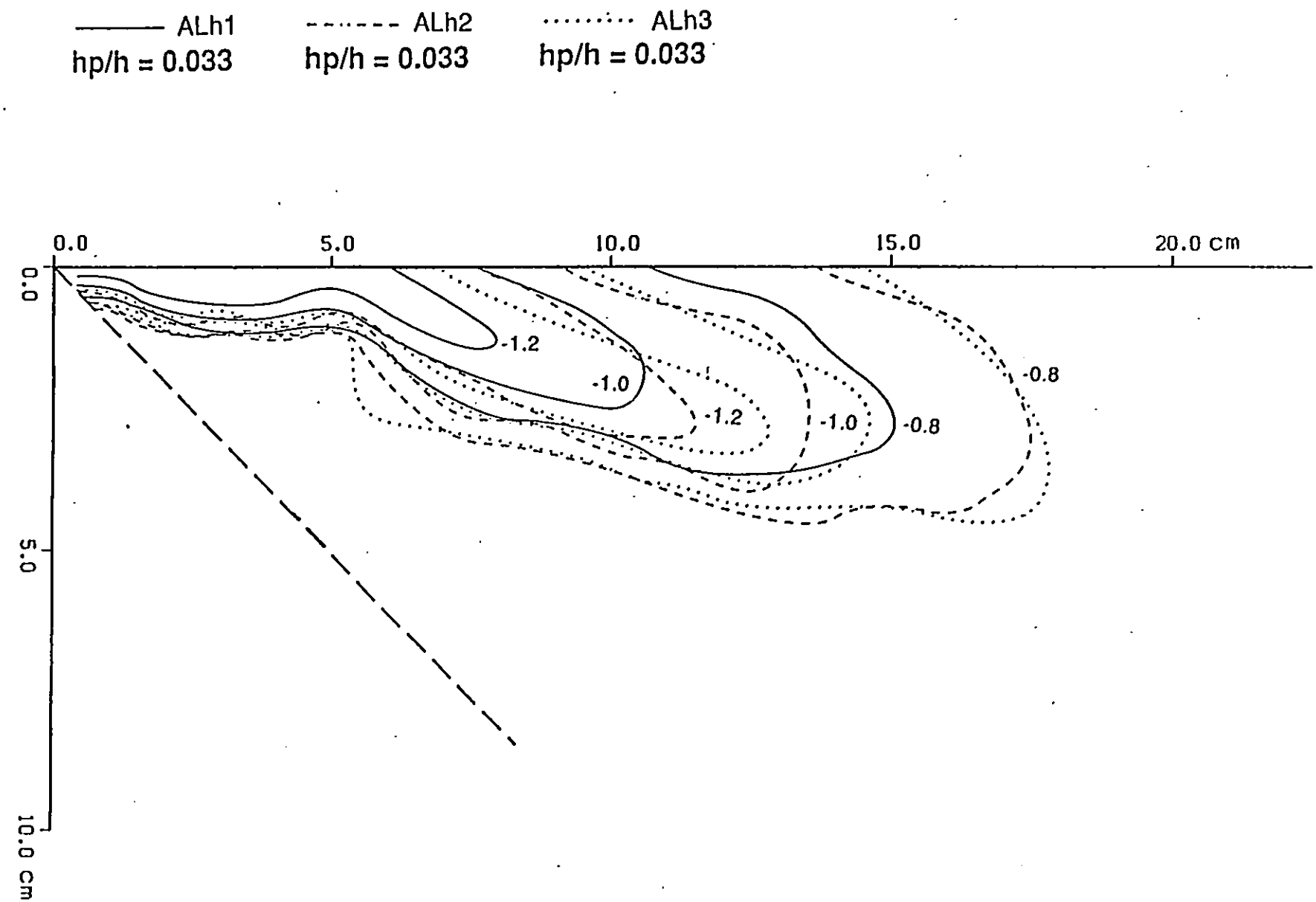

Figure 5.6: Mean Pressure Coefficients on Models with different Leights

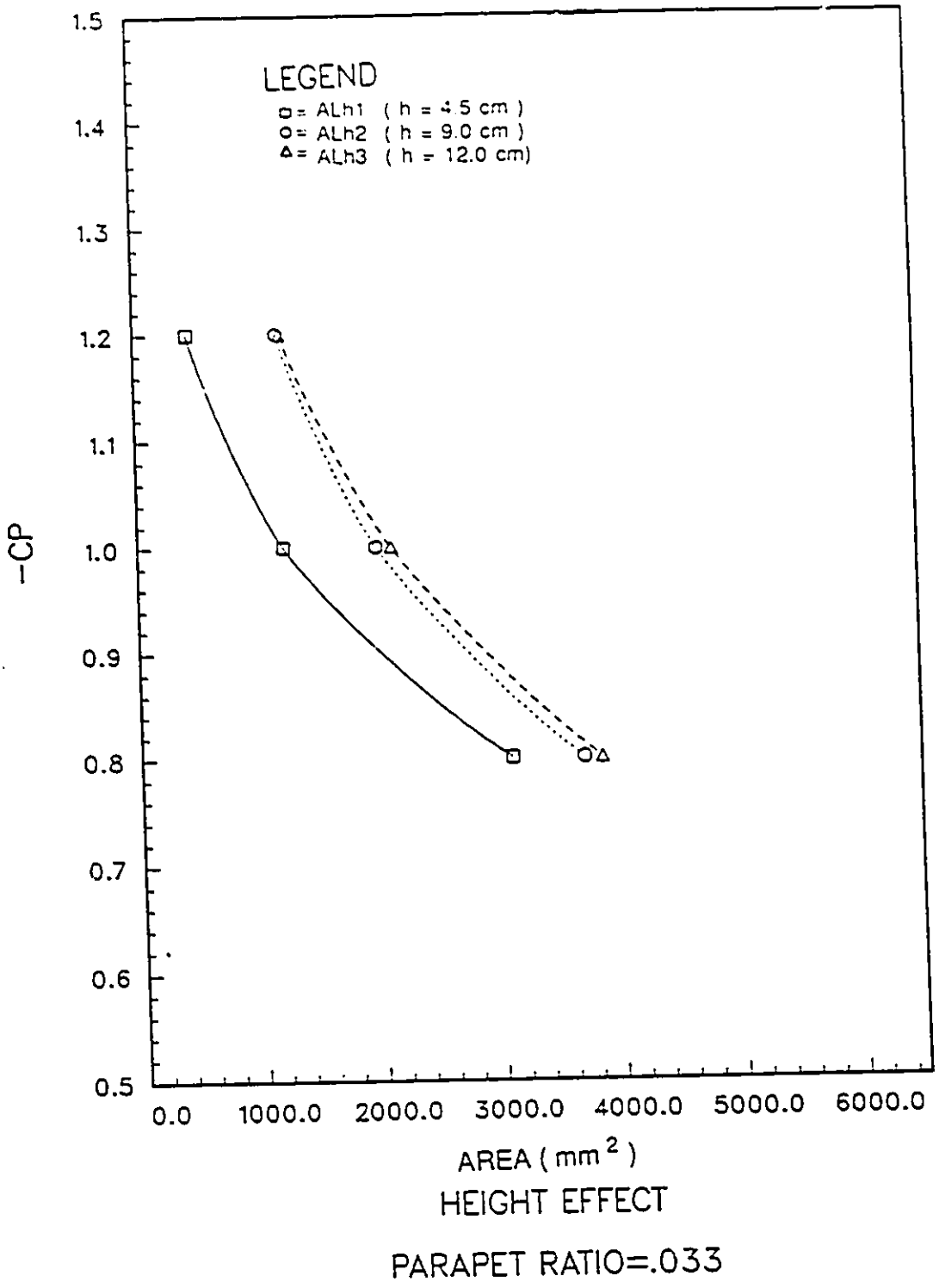

Figure 5.7: Height Effect on Mean Pressure Coefficient

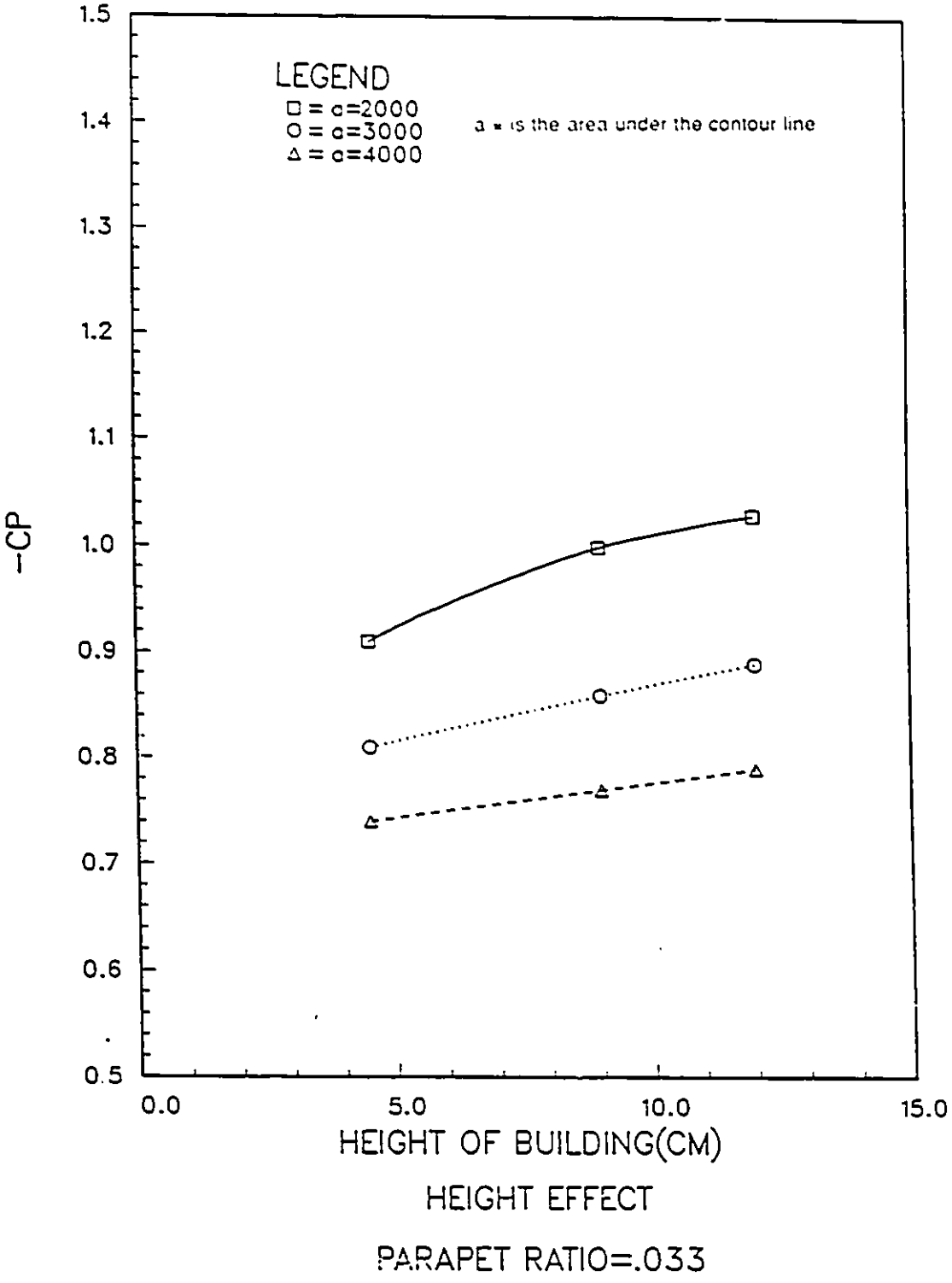

Figure 5.8: Height Effect on Mean Pressure Coefficient

5.4 Blockage Effects

The knowledge of blockage effects in any measurements at closed wind tunnel test sections is essential for making proper corrections for the results converted to unconstrained freestream conditions .

The blockage corrections depend mainly on the ratio of the projected model area normal to the flow over wind tunnel cross-section area, S/C, which reached up to 24% for the case of the model CH in our testing. The well known Maskell's theory [27] has derived the following correction formula for the drag force

$$\Delta q/q = \epsilon C_D S/C \tag{5.1}$$

where Δq is the effective increase in dynamic pressure due to constraint, q is the reference dynamic pressure,($= \frac{\rho V^2}{2}$) in upstream, ϵ is a blockage factor coefficient, C_D is the measured drag coefficient($= drag/qS$),S is the model reference area and C is the cross-sectional area of the closed wind tunnel test section. Unfortunately, the blockage effects on pressure on three dimensional bluff bodies are very complicated as reported by Melborne [28]. Measurements of peak pressure under reattaching shear layers, for example, are increasingly required by designers of buildings to determine cladding/glazing loads. And yet it is difficult to define proper blockage correction for this case. Melborne also showed [29] that the corrections for isolated plates also applicable to combinations of rectangular plates mounted side by side normal to the flow.

Also it has been shown that the linear form of blockage correction

$$\Delta C_p = C_p - C_{pc} = KC_D S/C \tag{5.2}$$

is applicable for the majority of both two and three dimensional model configurations. In Eq. 5.2 C_D is the measured drag coefficient based on reference area S. C is the wind tunnel cross-sectional area. C_{pc} is the pressure coefficient corrected to unbounded freestream conditions and K is a constant depending on model/flow/wind tunnel configurations. The empirical factor K is a function of the building height over upstream width expressed as h/b. Listed in Table 5.3 are some values of K for several h/b ratios [30].

Table 5.3: Empirical values of K

h/b	K
4	2.1
2	1.9
1	1.8
1/2	1.6

Unfortunately, no previous research is available regarding the blockage effects on the roof suction. However, blockage effect on side pressure is somehow a little more advanced especially for two dimensional plates. An assumption to extend the above mentioned blockage correction is needed for the roof suction correction. The following models are used for this analysis as shown in Table

5.4.

Table 5.4: Models tested for wind tunnel blockage effect

Model	Model area S(cm^2)	Blockage ratio S/C (%)	Parapet ratio h_p/h
ALW	153	1.8	.033
BHW	1086	13.0	.033
CH	1966	24.0	.033
CL	409	4.9	.033

The model CL is modified by changing the parapet ratio to 0.033 so that it can be compared with CH to know the wind tunnel blockage effect. Having the blockage ratio parameter different, a big difference in the results of CH and CL is observed which is a greater suction in CH of greater blockage as it is obvious in Fig. 5.9. However this deviation in results is due to, not only the blockage ratio effect but also to the scale proportionality caused by reducing the height and not the other dimensions. Better cases for this blockage analysis are ALW, BHW and CH.

ALW, BHW and CH correspond to three models of different scales of the same prototype and as observed in Chapt.4, ALW and BHW gave similar results but CH gave different results. This deviation can be considered as the blockage effect since all other parameters were kept invariant. By expressing this difference (ΔC_p) by the correction formula, where K is given for a specific h/b ratio, the only unknown is the drag force coefficient C_D supposed to be

measured. But since it was not the concern of this study, it can be calculated by the formula and then the blockage correction of any model can be computed. The question remains whether or not this correction formula can be applied for this case. Even if it is applicable, there is another question which is to what extent it can be true.

Fig. 5.11 presents the pressure coefficient as a function of blockage ratio as derived from Fig. 5.10. What can be observed from this is that no significant variation of the pressure coefficient with blockage ratio observed up to about the ratio of 15%. Right after this part of the curve, a big positive slope is observed and the same tendency is repeated in three curves, which means that C_p can be expressed by the similar way as a function of S/C.

The closest function to what is plotted is an exponential expression:

$$C_p = C_{pc} e^{K' S/C} \tag{5.3}$$

where K' is a constant depending on the drag force coefficient and the ratio of the building height to the upstream width, h/b.

After using a regression technique, K' was found to be 0.02 for all three curves. For more details, consult Appendix D. The relationship between K' and other parameters is not known yet.

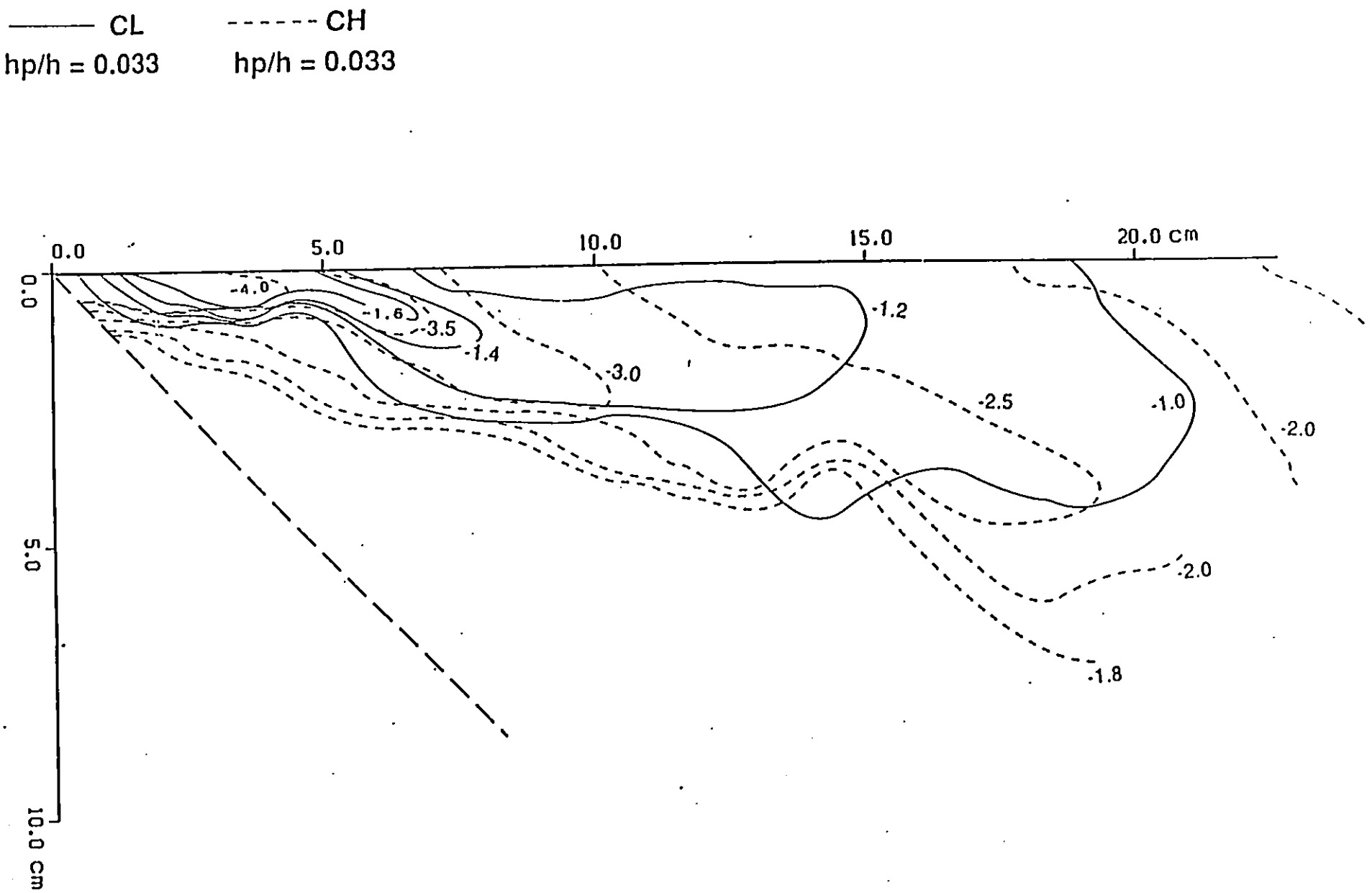

Figure 5.9: Mean Pressure Coefficients:CL and CH

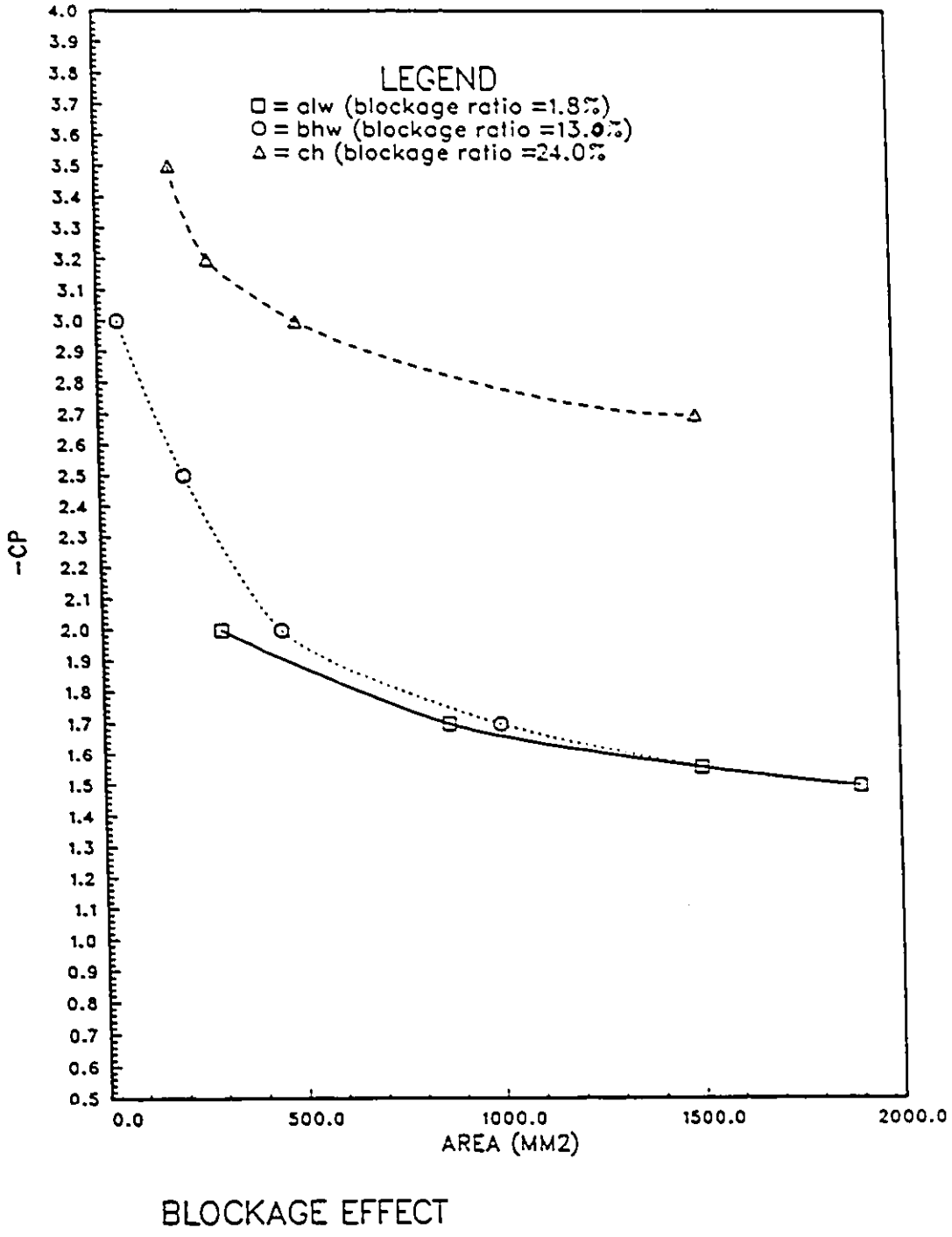

Figure 5.10: Effect of Blockage on Mean Pressure Coefficient

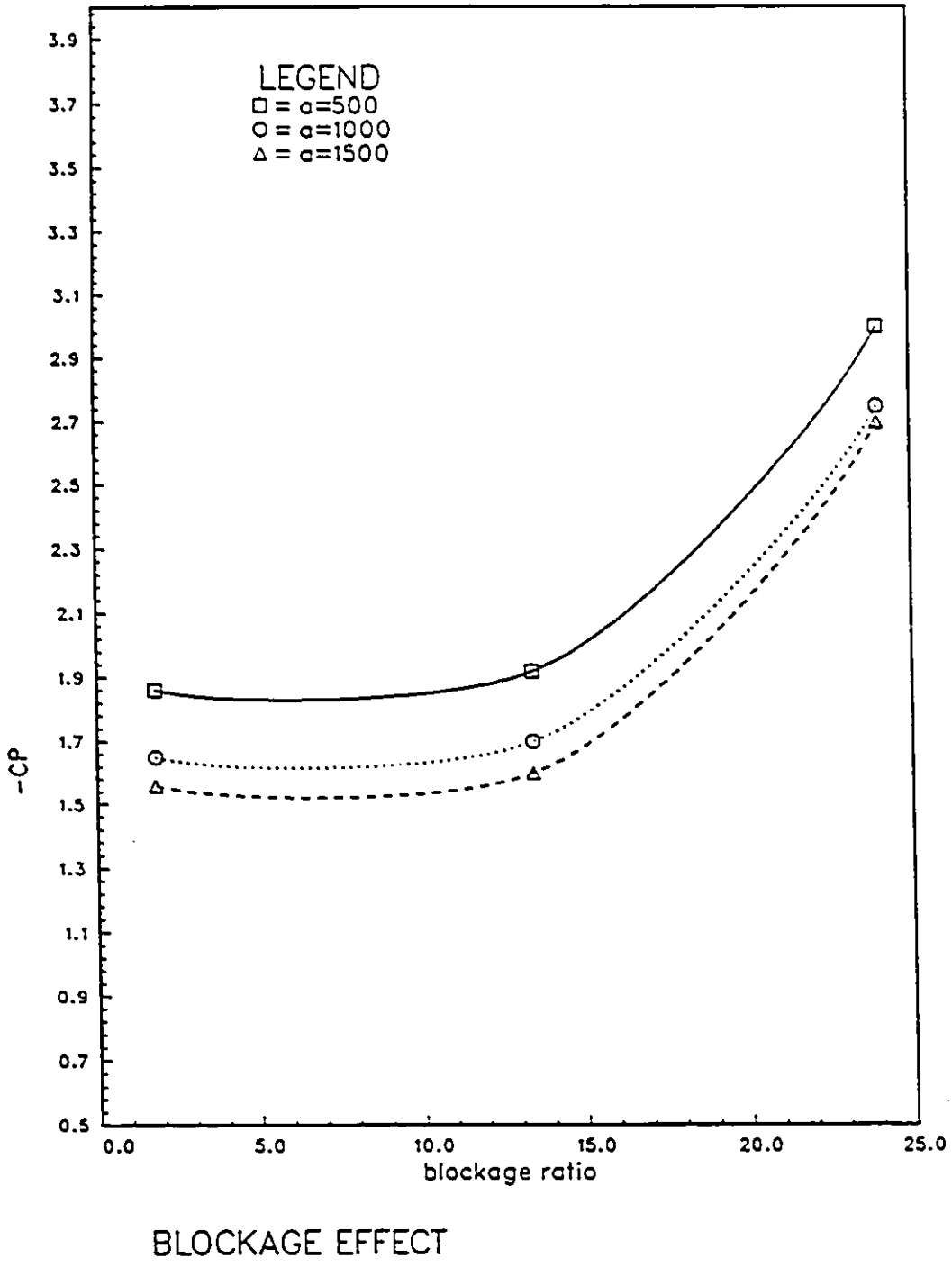

Figure 5.11: Effect of Blockage on Mean Pressure Coefficient

Chapter 6

Conclusions and Recommendations

A wind tunnel study for the determination of pressure distribution on flat roofs due to wind induced suction has been carried out.

Different building scales of various shapes of whole and half models have been examined. Mean pressure coefficients have been measured and analysed.

Furthermore, attempts have been made to better understand the effect of parapets, height of building and wind tunnel blockage by examining various building heights for a variety of roof parapets.

The experimental results indicated that the wind tunnel test of a 1/10-model of the previously tested building model in a 1/10-scaled wind tunnel gave a good agreement in wind induced roof pressure results.

Pressure distributions measured on a half model and a whole model are

comparable which identifies that the simulation of a small portion of the building can also simulate the wind induced pressure pattern on the roof deck.

Use of a plate along the line of symmetry of the building during the testing of a half model is recommendable.

Since the testing of a 1/10-scaled model in the $9m \times 9m$ wind tunnel and testing of a 1/100 model in the $0.9m \times 0.9m$ win tunnel have been found to give similar results, testing of 1/21 scale model in the small wind tunnel can similarly predict the test results of a 1/2 scale model in the large wind tunnel. The blockage effect which can be as high as up to about 25% can be taken into consideration. This will be a useful information for the examination of the mechanical characteristics of the structural details of the roof deck against strong wind induced suction.

The results of testing on parapet effect confirmed the previous studies at an extent that the parapets generally reduce the high suction at the roof edges and may slightly affect the loads acting on the internal areas of the roof. Roof corners, however, are affected differently. The suction at the corners increases rather than decreases. When the parapet height exceeds certain level, the tendancy was found to reverse. It is recommended for future work to examine this reversing effect in more details.

Finally for more accurate blockage correction, for the pressure over the flat roof deck of buildings more work is needed in future.

Bibliography

[1] KIND, R.J. "*Wind tunnel tests on some building models to measure wind speeds at which gravel is blown off roof tops*"., NRCC, Report LTR-LA-162 June 1974.

[2] KIND, R.J., "*Worst suctions near edges of flat rooftops on low-rise buildings* "., J. of Wind Engineering and Industrial Aerodynamics(25), 1986, pp. 31-47

[3] KIND, R.J. and WARDLAW, R.L., "*Failure mechanisms of loose-laid roof-insulation systems* "., J. of Wind Engineering and Industrial Aerodynamics(9), 1982, pp.325-341

[4] KIND, R.J., SAVAGE, M.G. and WARDLAW, R.L., "*Prediction of wind- induced failure of loose-laid roof cladding systems* ". J.of W.E and Industrial Aerodynamics 29 (1988) 29-37

[5] KIND, R.J., WARDLAW, R.L. and SAVAGE, M.G. , "*Wind effects on loose-laid cladding systems* ". Structures congress '89, ASCE, San Francisco, CA. May 1-5, 1989.

[6] BASKARAN, A. " *Wind loads on flat roofs with parapets*". M.Eng. Thesis, Center for Building Studies, Concordia University. Montreal, Québéc. Canada. April 1986.

[7] The CSU/TTU Cooperative Program Report.
Volume 1, Number1, Fall 1990.

[8] KIND, R.J. and WARDLAW, R.L., *"Behaviour in wind of loose-laid roof insulation systems.PartI Stone scour and blow-off "*.

[9] KIND, R.J. and WARDLAW, R.L., *"Design of rooftops against gravel blow-off "*., National Aeronautical Establishment, Ottawa, September 1976.

[10] KIND, R.J.*"Further wind tunnel tests on building models to measure wind speeds at which gravel is blown off roof tops "*.

[11] KIND, R.J. and WARDLAW, R.L., *"Behaviour in wind of loose-laid roof insulation systems.PartII Loose-laid membranes, paving slabs and insulation boards."*

[12] LEUTHEUSSER, H.J. *"The effect of wall parapets on the roof pressure coefficients of block-type and cylindrical structures "*. Technical Publication Series, No. TP6404, Department of Mechanical Engineering, University of Toronto, Toronto, Ontario, 1964.

[13] COLUMBUS, J. K. *"The study of pressure coefficients on large flat roofs and the effect of parapets on these coefficients "*. Engineering Science 400 report, The University of Western Ontario, London, Ont., 1972

[14] DAVENPORT A. G., and SURRY, D. *"The pressure on low-rise structures in turbulent wind "*. Proceedings of the Canadian Structural Engineering Conference, The Canadian Steel Industries Construction Council, Toronto, Ont., pp 1-39, 1974

[15] KRAMER, C., GERHARDT, H. J. and SCHERER, C. *"Wind pressure on block-type buildings "*. Proceedings of the 3rd Colloquium

on Industrial Aerodynamics, Aachen, West Germany, June 14-16, 1978

[16] SOCKEL, H. and TAUCHER, R. "*The influence of a parapet on local pressure fluctuations* ". Proceedings of the 4th Colloquium on Industrial Aerodynamics, Aachen, West Germany, June 18-20, 1980.

[17] STATHOPOULOS, T. "*Wind pressures on low buildings with parapets* ". ASCE Journal of the Structural Division, 108(12):2723-2736, 1982.

[18] LYTHE,G. and SURRY, D. "*Wind loading on flat roofs with and without parapets* ". Journal of Engineering and Industrial Aerodynamics, 11: 75-94, 1983.

[19] STATHOPOULOS, T. and BASKARAN, A. "*Wind Pressures on Flat Roofs with Parapets*". ASCE Journal of Structural Engineering, 113(11):2166-2180, Nov. 1987.

[20] STATHOPOULOS, T. and BASKARAN, A. "*Turbulent wind loading of roofs with parapet configurations*". Center for Building Studies, Concordia University, Montreal, Québéc, Canada, Jan. 1988.

[21] KIND, R. J. and WARDLAW, R.L. "*Model studies of the wind resistance of two loose-laid roof-insulation systems*". Laboratory Technical Report LTR-LA-234 May 1979.

[22] GERHARDT, H.J. *Wind loads on roofing systems-roof membranes, tiles and loose-laid slabs* ". Fluid mechanics laboratory, Fashhoschule, Aachen

[23] STATHOPOULOS, T., BASKARAN, A. and GOH, P.A. "*Full scale measurements of wind pressures on flat roof corners* ". Proceedings

of the sixth U.S. National Conference on Wind Engineering. Volume II, march 8-10 1989. University of Houston. Houst, Texas.

[24] KIND, R.J., SAVAGE, M.G. and WARDLAW, R.L *"Pressure distribution data measured during september 1986 wind tunnel tests on loose-laid roofing systems "*. Report LTR-LA-29, sept 1987.

[25] LEUTHESSER, HANS. J., *"Influence of architectural features on the static wind loading of buildings "*. Proceedings. Technical meeting concerning wind loads on buildings and structures. 1969. National Bureau of Standards, Gaithersburg, Maryland.

[26] NACY, P.S., *Modification of pressure distribution around buildings due to parapets "*. M.S Theses. Department of Mechanics and hydraulics. Graduate College, State university of IOWA, june 1951.

[27] MASKELL, E. C. *" A theory of the blockage effects on bluff bodies and stalled wings in a closed wind tunnel"*. Research and Memorandom No.3400, HMSO, London, 1963, also RAE report Aero.2685

[28] MELBORNE, W. H. *" Wind tunnel blockage effects and corrections"*. NBS/NSF Workshop on Wind Tunnel Modelling for Civil Engineering Applications, Gaithersburg, Maryland, April 1982.

[29] MCKEON, R. J. and MELBORNE, W. H. *" Wind tunnel blockage effects and drag on bluff bodies in a rough wall boundary layer"*., Proceeding of the 3rd International Conference on Wind Effects on Buildings and Structures , Tokyo, 263-272, 1971.

[30] Des Rosiers, P. P. *" Blockage effects in closed-throat wind tunnel testing"*. M.S Thesis, Department of Civil Engineering, Ottawa University. Ottawa, Ontario, 1982

Appendix A

Tabulated Data

GLN

PORT#	AVG.	RMS.	MAX.	MIN.	PORT#	AVG.	RMS.	MAX.	MIN.
ZERO	-0.122	0.041	0.018	-0.279	ZERO	-0.130	0.054	0.052	-0.298
DYN.	0.324	0.041	0.468	0.179	DYN.	0.290	0.053	0.507	0.127
1	-1.186	0.996	1.207	-5.920	47	-0.843	0.521	0.853	-2.888
2	-0.346	0.317	0.978	-1.576	48	-0.886	0.442	0.638	-2.424
3	-2.350	0.611	-0.646	-4.301	49	-0.803	0.396	0.482	-1.988
4	-0.258	0.287	0.736	-1.197	50	-0.742	0.382	0.465	-2.177
5	-1.299	0.690	0.819	-3.559	51	-0.128	0.347	1.056	-1.370
ZERO	-0.122	0.042	0.032	-0.264	ZERO	-0.133	0.053	0.033	-0.307
DYN.	0.322	0.042	0.442	0.169	DYN.	0.293	0.053	0.477	0.130
6	-1.610	0.450	-0.087	-3.652	52	-0.121	0.358	1.194	-1.532
7	-0.233	0.277	0.880	-1.049	53	-0.094	0.376	1.378	-1.537
8	-0.445	0.459	0.930	-2.978	54	-0.211	0.447	1.221	-1.955
9	-1.690	0.506	0.536	-3.643	55	-0.720	0.484	0.893	-2.560
10	-1.370	0.405	-0.178	-2.868	56	-0.923	0.450	0.576	-2.666
ZERO	-0.118	0.041	0.008	-0.252	ZERO	-0.131	0.053	0.055	-0.312
DYN.	0.317	0.042	0.446	0.171	DYN.	0.290	0.053	0.445	0.127
11	-0.261	0.276	0.790	-1.143	57	-0.806	0.410	0.565	-2.350
12	-0.251	0.318	0.893	-2.079	58	-0.754	0.396	0.520	-2.119
13	-1.603	0.519	0.421	-3.948	59	-0.144	0.353	1.172	-1.636
14	-1.149	0.360	-0.029	-2.345	60	-0.114	0.358	1.082	-1.252
15	-0.181	0.275	0.672	-1.103	61	-0.093	0.364	0.978	-1.629
ZERO	-0.123	0.041	-0.004	-0.259	ZERO	-0.133	0.053	0.052	-0.335
DYN.	0.321	0.042	0.462	0.201	DYN.	0.286	0.053	0.462	0.083
16	-0.524	0.521	0.813	-2.928	62	0.191	0.434	1.125	-1.753
17	-1.256	0.424	0.062	-2.652	63	-0.637	0.467	0.711	-2.332
18	-1.126	0.375	0.111	-2.466	64	-0.836	0.453	0.503	-2.479
19	-1.023	0.348	0.311	-2.304	65	-0.790	0.403	0.554	-2.098
20	-0.137	0.270	0.593	-1.140	66	-0.732	0.401	0.512	-2.908
ZERO	-0.123	0.042	0.018	-0.258	ZERO	-0.130	0.052	0.047	-0.315
DYN.	0.321	0.042	0.449	0.191	DYN.	0.286	0.052	0.488	0.127
21	-0.162	0.307	0.970	-2.190	67	-0.660	0.379	0.645	-1.959
22	-0.945	0.567	0.971	-3.030	68	-0.138	0.358	1.055	-1.137
23	-1.102	0.391	0.195	-2.752	69	-0.141	0.366	0.978	-1.237
24	-0.942	0.332	0.074	-2.104	70	-0.061	0.367	1.255	-1.210
25	-0.163	0.270	0.641	-0.969	71	-0.103	0.404	1.641	-1.572
ZERO	-0.126	0.042	0.022	-0.276	ZERO	-0.132	0.053	0.074	-0.281
DYN.	0.324	0.042	0.469	0.146	DYN.	0.282	0.054	0.478	0.087
26	-0.126	0.256	0.749	-1.001	72	-0.379	0.453	1.156	-1.972
27	-0.243	0.35[illegible]	0.689	-1.997	73	-0.695	0.463	0.711	-2.003
28	-1.166	0.48[illegible]	0.251	-2.816	74	-0.721	0.407	0.587	-1.927
29	-1.000	0.36[illegible]	0.165	-2.656	75	-0.661	0.392	0.498	-2.131
30	-0.921	0.324	0.061	-2.118	76	-0.589	0.386	0.687	-2.022
ZERO	-0.127	0.042	0.019	-0.275	ZERO	-0.130	0.053	0.056	-0.289
DYN.	0.320	0.042	0.474	0.175	DYN.	0.289	0.053	0.445	0.116
31	-0.139	0.270	0.810	-1.134	77	-0.140	0.355	1.068	-1.430
32	-0.148	0.287	1.017	-1.143	78	-0.150	0.363	1.021	-1.451
33	-0.532	0.489	1.149	-2.455	79	-0.283	0.428	1.214	-2.227
34	-1.111	0.415	0.208	-3.550	80	-0.550	0.453	0.966	-2.095
35	-0.937	0.345	0.068	-2.281	81	-0.701	0.430	0.731	-2.279
ZERO	-0.123	0.043	0.019	-0.257	ZERO	-0.127	0.053	0.057	-0.337
DYN.	0.325	0.042	0.455	0.167	DYN.	0.285	0.054	0.454	0.076
36	-0.859	0.317	0.244	-1.853	82	-0.706	0.396	0.629	-1.927

37	-0.163	0.259	0.361	-1.211	83	-0.540	0.403	0.745	-2.271
38	-0.172	0.280	0.338	-1.479	84	-0.606	0.397	0.523	-1.946
39	-0.163	0.323	0.909	-1.592	85	-0.143	0.362	0.362	-1.399
40	-0.677	0.493	0.710	-3.000	86	-0.103	0.366	1.184	-1.471
ZERO	-0.116	0.042	0.030	-0.263	ZERO	-0.128	0.053	0.065	-0.314
DYN.	0.322	0.041	0.467	0.185	DYN.	0.285	0.053	0.449	0.077
41	-1.040	0.396	0.165	-2.479	87	-0.077	0.370	1.208	-1.249
42	-0.948	0.347	0.164	-2.091	88	-0.184	0.401	1.277	-1.476
43	-0.835	0.305	0.156	-1.826	89	-0.417	0.445	1.352	-2.293
44	-0.202	0.275	0.643	-1.144	90	-0.611	0.403	0.580	-2.284
45	-0.144	0.298	0.939	-1.177	91	-0.504	0.381	0.552	-1.833
ZERO	-0.115	0.041	0.025	-0.229	ZERO	-0.135	0.054	0.047	-0.290
DYN.	0.323	0.044	0.478	0.180	DYN.	0.288	0.052	0.468	0.119
46	-0.340	0.304	0.833	-2.347	92	-0.471	0.403	0.664	-2.150
ZERO	-0.123	0.041	0.000	-0.258	ZERO	-0.130	0.055	0.099	-0.349
DYN.	0.319	0.042	0.454	0.166	DYN.	0.288	0.054	0.494	0.092

TEMP 24.1DEG C. PRESS 101.2kPa. VEL 8.2m/sec. 8.3m/sec.

ALH

PORT=	AVG.	RMS.	MAX.	MIN.	PORT=	AVG.	RMS.	MAX.	MIN.
ZERO	-0.088	0.040	0.044	-0.229	ZERO	-0.088	0.053	0.130	-0.243
DYN.	0.356	0.042	0.500	0.191	DYN.	0.329	0.053	0.537	0.125
1	-1.936	0.398	1.527	-5.345	47	-0.825	0.479	0.639	-2.475
2	-0.965	0.891	1.447	-3.855	48	-0.867	0.430	0.356	-2.232
3	-1.750	0.519	-0.190	-3.461	49	-0.777	0.392	0.580	-2.188
4	-0.482	0.646	1.048	-4.329	50	-0.701	0.390	0.444	-1.989
5	-1.582	0.632	0.782	-3.301	51	-0.094	0.372	1.028	-1.430
ZERO	-0.094	0.041	0.047	-0.241	ZERO	-0.098	0.052	0.096	-0.279
DYN.	0.361	0.041	0.492	0.220	DYN.	0.334	0.052	0.519	0.164
6	-1.374	0.458	-0.105	-3.153	52	-0.055	0.362	1.129	-1.332
7	-0.221	0.441	1.026	-3.239	53	-0.052	0.371	1.188	-1.448
8	-0.689	0.644	0.822	-3.072	54	-0.286	0.469	1.432	-2.151
9	-1.458	0.485	-0.185	-3.578	55	-0.763	0.498	0.938	-2.407
10	-1.184	0.413	-0.047	-2.787	56	-0.839	0.442	0.897	-2.461
ZERO	-0.097	0.041	0.033	-0.229	ZERO	-0.090	0.054	0.094	-0.276
DYN.	0.351	0.042	0.498	0.205	DYN.	0.323	0.054	0.517	0.155
11	-0.110	0.344	0.997	-1.611	57	-0.786	0.413	0.649	-2.160
12	-0.300	0.462	1.098	-2.273	58	-0.711	0.402	0.731	-1.867
13	-1.343	0.453	0.191	-3.417	59	-0.048	0.360	1.146	-1.104
14	-0.970	0.368	0.179	-2.363	60	-0.013	0.355	1.160	-1.162
15	-0.082	0.311	0.780	-1.278	61	-0.051	0.390	1.273	-1.571
ZERO	-0.095	0.042	0.046	-0.254	ZERO	-0.100	0.052	0.083	-0.298
DYN.	0.347	0.043	0.485	0.219	DYN.	0.321	0.054	0.491	0.144
16	-0.656	0.594	1.430	-3.135	62	-0.287	0.450	1.326	-2.083
17	-1.175	0.419	0.345	-2.809	63	-0.639	0.479	0.829	-2.216
18	-0.986	0.364	0.238	-2.345	64	-0.733	0.430	0.793	-2.336
19	-0.925	0.355	0.213	-2.284	65	-0.685	0.412	0.476	-2.337
20	-0.124	0.299	0.930	-1.484	66	-0.642	0.410	1.672	-2.603
ZERO	-0.092	0.043	0.057	-0.249	ZERO	-0.100	0.055	0.093	-0.284
DYN.	0.352	0.042	0.536	0.209	DYN.	0.320	0.053	0.502	0.107
21	-0.163	0.401	1.340	-2.935	67	-0.686	0.385	0.673	-2.067
22	-1.034	0.523	0.744	-2.948	68	-0.062	0.361	1.376	-1.248
23	-1.148	0.391	0.048	-2.777	69	-0.031	0.364	1.136	-1.208
24	-0.922	0.348	0.173	-2.392	70	-0.023	0.365	1.219	-1.300
25	-0.110	0.301	0.875	-1.484	71	-0.136	0.410	1.117	-1.713
ZERO	-0.091	0.041	0.070	-0.211	ZERO	-0.105	0.055	0.086	-0.263
DYN.	0.351	0.041	0.484	0.218	DYN.	0.319	0.053	0.491	0.131
26	-0.078	0.298	0.923	-1.405	72	-0.383	0.453	0.997	-2.157
27	-0.365	0.455	0.895	-2.517	73	-0.643	0.452	0.912	-2.334
28	-1.094	0.463	0.350	-3.133	74	0.693	0.414	0.735	-2.110
29	-0.966	0.344	0.082	-2.238	75	-0.639	0.400	0.662	-2.089
30	-0.859	0.329	0.086	-1.932	76	-0.602	0.402	0.616	-2.082
ZERO	-0.095	0.042	0.057	-0.251	ZERO	-0.104	0.053	0.058	-0.298
DYN.	0.348	0.042	0.471	0.221	DYN.	0.315	0.054	0.486	0.119
31	-0.107	0.284	0.793	-1.073	77	-0.040	0.368	1.253	-1.442
32	-0.126	0.326	0.889	-1.434	78	-0.025	0.372	1.245	-1.414
33	-0.586	0.498	0.816	-2.947	79	-0.244	0.429	1.105	-1.784
34	-1.081	0.407	0.236	-2.607	80	-0.490	0.443	0.873	-1.942
35	-0.887	0.345	0.194	-2.197	81	-0.594	0.418	1.117	-2.205

ZERO	-0.097	0.041	0.034	-0.223	ZERO	-0.110	0.052	0.059	-0.283
DYN.	0.347	0.042	0.477	0.211	DYN	0.310	0.054	0.488	0.128
36	-0.750	0.309	0.208	-1.769	82	-0.587	0.399	0.806	-2.065
37	-0.091	0.292	0.798	-1.129	83	-0.570	0.393	0.681	-2.018
38	-0.053	0.286	1.006	-1.311	84	-0.540	0.397	0.748	-2.111
39	-0.146	0.359	1.095	-1.578	85	-0.039	0.350	0.961	-1.164
40	-0.678	0.460	0.637	-2.206	86	-0.057	0.364	1.194	-1.349
ZERO	-0.104	0.041	0.023	-0.225	ZERO	-0.110	0.054	0.090	-0.302
DYN.	0.350	0.041	0.493	0.211	DYN.	0.309	0.053	0.492	0.133
41	-0.926	0.381	0.448	-2.573	87	-0.053	0.370	1.269	-1.517
42	-0.781	0.313	0.269	-2.050	88	-0.152	0.405	1.099	-1.756
43	-0.700	0.309	0.376	-1.858	89	-0.373	0.424	1.081	-1.718
44	-0.062	0.281	1.321	-0.833	90	-0.564	0.415	0.951	-1.806
45	-0.056	0.300	1.120	-1.121	91	-0.514	0.385	0.782	-1.853
ZERO	-0.104	0.042	0.030	-0.246	ZERO	-0.113	0.053	0.048	-0.299
DYN.	0.341	0.041	0.488	0.205	DYN.	0.309	0.052	0.482	0.118
46	-0.311	0.414	0.950	-1.715	92	-0.487	0.403	0.985	-2.848
ZERO	-0.102	0.043	0.031	-0.267	ZERO	-0.113	0.054	0.061	-0.268
DYN.	0.341	0.042	0.487	0.207	DYN.	0.306	0.054	0.495	0.114

TEMP 23.5DEG C. PRESS 101.0kPa. VEL 8.3m/sec. 8.3m/sec.

PORT=	AVG.	RMS.	MAX.	MIN.	PORT=	AVG.	RMS.	MAX.	MIN.
ZERO	-0.075	0.042	0.073	-0.205	ZERO	-0.069	0.054	0.113	-0.281
DYN.	0.244	0.042	0.382	0.088	DYN.	0.226	0.053	0.429	0.052
1	-4.399	1.413	1.546	-7.552	47	-1.536	0.614	1.093	-3.489
2	-0.148	0.553	1.390	-5.147	48	-1.623	0.517	0.057	-3.527
3	-3.204	0.611	-1.173	-5.229	49	1.497	0.481	0.042	-3.239
4	-0.204	0.297	1.078	-1.174	50	-1.262	0.457	0.355	-2.680
5	-2.532	0.761	-0.155	-5.275	51	-0.159	0.365	1.140	-1.442
ZERO	-0.068	0.041	0.063	-0.203	ZERO	-0.061	0.053	0.106	-0.231
DYN.	0.251	0.042	0.415	0.118	DYN.	0.226	0.054	0.380	0.040
6	-2.723	0.650	-0.794	-5.256	52	-0.147	0.366	1.020	-1.321
7	-0.147	0.279	0.837	-1.166	53	-0.104	0.383	1.239	-1.269
8	-0.622	0.548	0.782	-4.097	54	-0.318	0.484	1.279	-2.378
9	-2.681	0.520	-1.169	-4.709	55	-1.418	0.594	0.507	-3.606
10	-2.171	0.546	-0.542	-4.169	56	-1.541	0.497	0.224	-3.375
ZERO	-0.067	0.042	0.074	-0.201	ZERO	-0.066	0.053	0.098	-0.255
DYN.	0.246	0.043	0.386	0.110	DYN.	0.239	0.054	0.411	0.046
11	-0.163	0.276	0.753	-1.033	57	-1.338	0.442	0.152	-2.767
12	-0.182	0.305	0.891	-1.203	58	-1.140	0.405	0.011	-2.424
13	-2.226	0.468	-0.927	-3.972	59	-0.123	0.353	1.057	-1.318
14	-1.670	0.430	-0.117	-3.256	60	-0.095	0.353	1.050	-1.292
15	-0.128	0.276	0.787	-1.190	61	-0.023	0.366	1.081	-1.332
ZERO	-0.069	0.042	0.071	-0.194	ZERO	-0.062	0.052	0.131	-0.247
DYN.	0.251	0.042	0.383	0.111	DYN.	0.238	0.054	0.405	0.084
16	-0.723	0.551	0.695	-3.640	62	-0.286	0.464	1.054	-2.749
17	-1.809	0.450	-0.070	-3.471	63	-1.214	0.621	0.720	-3.674
18	-1.796	0.417	-0.159	-3.573	64	-1.594	0.500	-0.062	-5.027
19	-1.713	0.447	0.173	-3.495	65	-1.423	0.474	0.412	-3.093
20	-0.148	0.268	0.704	-0.946	66	-1.272	0.427	0.184	-2.716
ZERO	-0.068	0.042	0.126	-0.207	ZERO	-0.057	0.052	0.114	-0.236
DYN.	0.247	0.042	0.378	0.087	DYN.	0.232	0.053	0.408	0.060
21	-0.184	0.304	0.890	-1.295	67	-1.257	0.441	0.189	-2.731
22	-1.452	0.633	0.549	-3.590	68	-0.190	0.357	1.110	-1.222
23	-1.792	0.455	-0.243	-3.772	69	-0.164	0.371	1.048	-1.356
24	-1.450	0.408	0.203	-2.805	70	-0.089	0.373	1.081	-1.233
25	-0.148	0.266	0.719	-1.007	71	-0.118	0.411	1.215	-2.354
ZERO	-0.066	0.043	0.066	-0.206	ZERO	-0.066	0.054	0.137	-0.224
DYN.	0.239	0.043	0.368	0.073	DYN.	0.230	0.053	0.449	0.037
26	-0.186	0.282	0.941	-1.099	72	-0.693	0.578	1.128	-2.978
27	-0.361	0.371	0.863	-2.002	73	-1.480	0.528	0.311	-3.367
28	-1.762	0.493	-0.374	-3.603	74	-1.384	0.499	0.138	-3.100
29	-1.650	0.441	-0.209	-3.448	75	-1.225	0.441	0.252	-2.893
30	-1.520	0.407	-0.026	-3.091	76	-1.168	0.426	0.213	-2.511
ZERO	-0.069	0.041	0.071	-0.198	ZERO	-0.067	0.053	0.098	-0.231
DYN.	0.245	0.040	0.368	0.108	DYN.	0.229	0.053	0.406	0.062
31	-0.189	0.266	0.804	-1.175	77	-0.164	0.356	1.083	-1.327
32	-0.166	0.295	1.093	-1.345	78	-0.123	0.366	1.221	-1.176
33	-0.776	0.534	0.699	-2.820	79	-0.302	0.451	1.238	-2.086
34	-1.748	0.433	-0.217	-4.115	80	-1.015	0.601	0.779	-2.997
35	-1.569	0.413	-0.341	-3.131	81	-1.558	0.517	0.190	-3.323
ZERO	-0.073	0.043	0.063	-0.213	ZERO	-0.070	0.054	0.103	-0.233
DYN.	0.239	0.041	0.366	0.095	DYN.	0.225	0.053	0.411	0.059
36	-1.301	0.382	0.155	-2.733	82	-1.326	0.458	0.096	-3.616

37	-0.181	0.271	0.724	-1.114	83	-1.164	0.422	0.058	-2.937
38	-0.111	0.271	0.771	-0.996	84	-1.081	0.427	0.553	-2.633
39	-0.162	0.316	0.813	-1.748	85	-0.120	0.356	1.311	-1.270
40	-1.247	0.584	0.509	-2.950	86	-0.103	0.378	0.937	-1.289
ZERO	-0.076	0.040	0.074	-0.202	ZERO	-0.072	0.054	0.105	-0.245
DYN.	0.237	0.041	0.362	0.083	DYN.	0.221	0.053	0.392	0.040
41	-1.673	0.470	-0.147	-3.905	87	-0.074	0.375	1.248	-1.154
42	-1.422	0.389	-0.133	-3.109	88	-0.149	0.434	1.279	-1.984
43	-1.308	0.379	0.036	-3.026	89	-0.886	0.609	0.898	-2.889
44	-0.113	0.266	0.717	-1.126	90	-1.496	0.505	0.531	-3.448
45	-0.062	0.278	0.762	-0.977	91	-1.210	0.442	0.159	-2.775
ZERO	-0.082	0.042	0.079	-0.228	ZERO	-0.076	0.054	0.110	-0.286
DYN.	0.243	0.041	0.378	0.101	DYN.	0.219	0.052	0.381	0.037
46	-0.400	0.409	1.194	-2.770	92	-1.143	0.407	0.250	-2.652
ZERO	-0.077	0.042	0.050	-0.220	ZERO	-0.078	0.053	0.104	-0.233
DYN.	0.231	0.041	0.360	0.096	DYN.	0.214	0.054	0.466	0.029

TEMP 22.9DEG C. PRESS 98.7kPa. VEL 7.0m/sec. 7.0m/sec.
PROFILE RATIO 0.710

CH

PORT#	AVG.	RMS.	MAX.	MIN.	PORT#	AVG.	RMS.	MAX.	MIN.
ZERO	-0.001	0.042	0.121	-0.134	ZERO	0.015	0.052	0.171	-0.191
DYN.	0.264	0.042	0.431	0.104	DYN.	0.270	0.054	0.439	0.100
1	-4.054	0.752	-1.717	-7.249	47	-3.841	0.602	-0.354	-4.784
2	-4.418	1.470	2.434	-9.479	48	-3.647	0.605	-0.421	-5.428
3	-4.770	0.745	-2.196	-7.313	49	-3.432	0.524	-0.514	-4.681
4	-0.686	1.367	2.782	-5.639	50	-3.002	0.507	-0.393	-4.439
5	-4.621	0.996	-1.000	-8.696	51	-0.534	0.350	0.550	-1.678
ZERO	-0.009	0.041	0.136	-0.138	ZERO	0.023	0.052	0.202	-0.178
DYN.	0.267	0.042	0.405	0.137	DYN.	0.277	0.054	0.448	0.111
6	-3.952	0.690	-1.590	-6.756	52	-0.444	0.349	0.741	-1.482
7	-0.346	0.553	2.099	-3.478	53	-0.385	0.405	1.151	-1.723
8	-2.233	1.264	0.626	-7.695	54	-1.092	0.668	0.718	-3.993
9	-4.336	0.595	-2.458	-7.212	55	-2.724	0.593	-0.630	-5.181
10	-3.694	0.662	-0.559	-5.977	56	-2.590	0.594	-0.532	-6.004
ZERO	0.002	0.041	0.153	-0.140	ZERO	0.029	0.053	0.223	-0.142
DYN.	0.265	0.042	0.440	0.107	DYN.	0.287	0.053	0.471	0.113
11	-0.404	0.353	1.108	-1.349	57	-2.293	0.536	-0.515	-4.683
12	-1.018	0.719	0.701	-5.193	58	-2.068	0.455	0.121	-3.866
13	-4.236	0.548	-2.195	-6.533	59	-0.529	0.353	0.609	-1.819
14	-3.123	0.629	-0.915	-5.193	60	-0.398	0.375	0.829	-1.647
15	-0.468	0.319	0.631	-1.917	61	0.427	0.401	0.972	-1.959
ZERO	0.002	0.043	0.158	-0.171	ZERO	0.035	0.053	0.219	-0.163
DYN.	0.266	0.041	0.395	0.139	DYN.	0.284	0.054	0.446	0.104
16	-2.278	0.996	0.638	-5.071	62	-1.234	0.701	0.680	-4.031
17	-3.563	0.536	-1.835	-6.402	63	-2.623	0.639	-0.348	-5.603
18	-3.332	0.601	-0.417	-6.272	64	-2.678	0.624	-0.696	-5.276
19	-2.774	0.617	-0.381	-5.115	65	-2.427	0.546	0.454	-5.429
20	-0.402	0.281	0.538	-1.380	66	-2.189	0.474	-0.149	-4.239
ZERO	-0.008	0.042	0.119	-0.165	ZERO	0.035	0.052	0.209	-0.123
DYN.	0.263	0.042	0.406	0.131	DYN.	0.286	0.054	0.467	0.101
21	-0.604	0.409	1.444	-2.794	67	-1.985	0.454	-0.057	-3.396
22	-3.146	0.829	-0.509	-5.389	68	-0.538	0.355	0.626	-1.829
23	-3.258	0.610	-1.254	-5.845	69	-0.441	0.364	0.923	-1.761
24	-2.612	0.652	-0.529	-4.978	70	-0.323	0.406	1.439	-1.805
25	-0.518	0.292	0.469	-1.372	71	-0.720	0.577	0.940	-3.231
ZERO	0.004	0.043	0.136	-0.157	ZERO	0.035	0.053	0.193	-0.132
DYN.	0.254	0.041	0.374	0.105	DYN.	0.283	0.053	0.461	0.130
26	-0.517	0.337	1.348	-1.760	72	-1.883	0.737	0.362	-4.091
27	-1.176	0.628	0.700	-4.506	73	-2.800	0.577	-1.030	-4.609
28	-3.619	0.586	-1.749	-5.767	74	-2.428	0.593	-0.563	-4.937
29	-3.132	0.601	-1.349	-5.528	75	-2.092	0.480	-0.721	-4.620
30	-2.313	0.539	-0.447	-4.362	76	-1.930	0.473	-0.214	-5.249
ZERO	-0.001	0.043	0.134	-0.149	ZERO	0.033	0.053	0.204	-0.140
DYN.	0.260	0.043	0.398	0.107	DYN.	0.279	0.053	0.511	0.119
31	-0.588	0.285	0.474	-1.567	77	-0.445	0.360	0.801	-1.611
32	-0.514	0.374	0.850	-2.009	78	-0.349	0.284	0.888	-1.663
33	-1.992	0.765	0.163	-4.358	79	-1.253	0.718	0.861	-3.960
34	-3.282	0.585	-1.405	-5.794	80	-2.440	0.687	-0.177	-5.230
35	-2.801	0.525	-0.346	-4.729	81	-2.575	0.615	-0.803	-5.214
ZERO	-0.003	0.042	0.130	-0.137	ZERO	0.033	0.053	0.209	-0.178
DYN.	0.261	0.042	0.389	0.099	DYN.	0.290	0.053	0.451	0.111
36	-2.331	0.503	-0.567	-4.678	82	-2.147	0.504	-0.597	-4.486

37	-0.572	0.280	0.425	-1.472	83	-2.000	0.437	-0.420	-3.511
38	-0.449	0.297	0.601	-1.497	84	-1.859	0.440	-0.356	-3.202
39	-0.741	0.504	0.877	-4.177	85	-0.522	0.357	0.656	-1.722
40	-2.560	0.714	-0.223	-4.728	86	-0.436	0.358	0.789	-1.490
ZERO	-0.004	0.043	0.134	-0.132	ZERO	0.029	0.055	0.198	-0.140
DYN.	0.259	0.641	0.394	0.127	DYN.	0.280	0.053	0.470	0.077
41	-2.937	0.561	-0.598	-5.068	87	-0.368	0.374	0.855	-1.670
42	-2.697	0.510	-0.960	-4.721	88	-0.750	0.575	0.959	-3.729
43	-2.267	0.495	-0.218	-3.878	89	-2.192	0.689	-0.021	-4.982
44	-0.439	0.282	0.494	-1.311	90	-2.419	0.628	-0.431	-5.160
45	-0.334	0.313	0.752	-1.384	91	-1.974	0.472	-0.467	-3.488
ZERO	0.000	0.043	0.125	-0.164	ZERO	0.043	0.053	0.212	-0.127
DYN.	0.269	0.041	0.416	0.136	DYN.	0.293	0.053	0.468	0.143
46	-1.072	0.627	0.560	-3.740	92	-1.729	0.436	-0.417	-3.157
ZERO	0.002	0.043	0.146	-0.132	ZERO	0.043	0.053	0.210	-0.124
DYN.	0.272	0.042	0.428	0.142	DYN.	0.293	0.053	0.467	0.101

TEMP 23.6DEG C. PRESS 100.2kPa. VEL 6.4m/sec. 6.4m/sec.
PROFILE RATIO 0.780

Appendix B

Models in the wind tunnel

Figure B.1: Model AMW

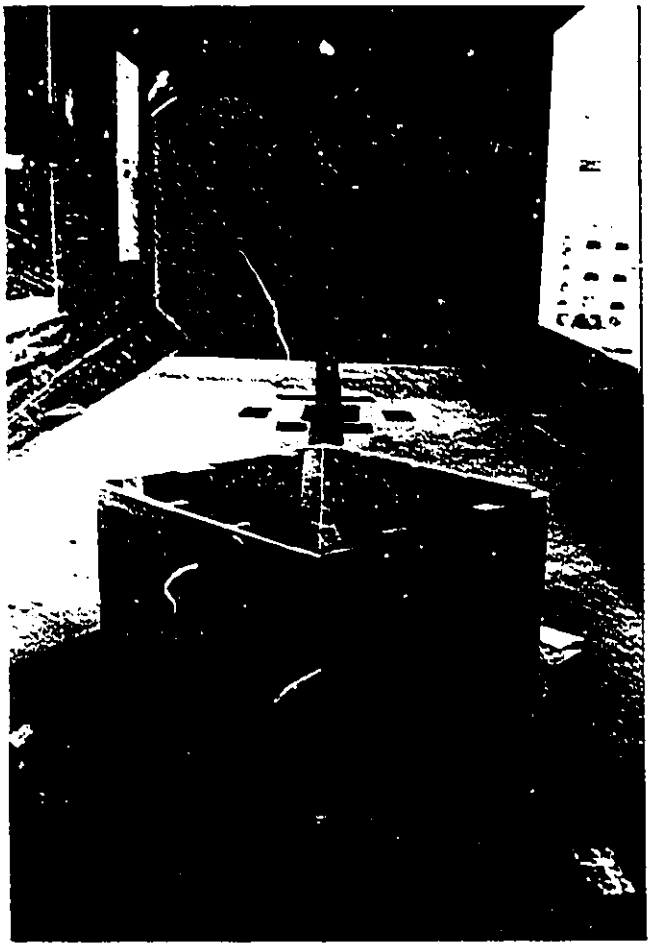

Figure B.2: Model AHW

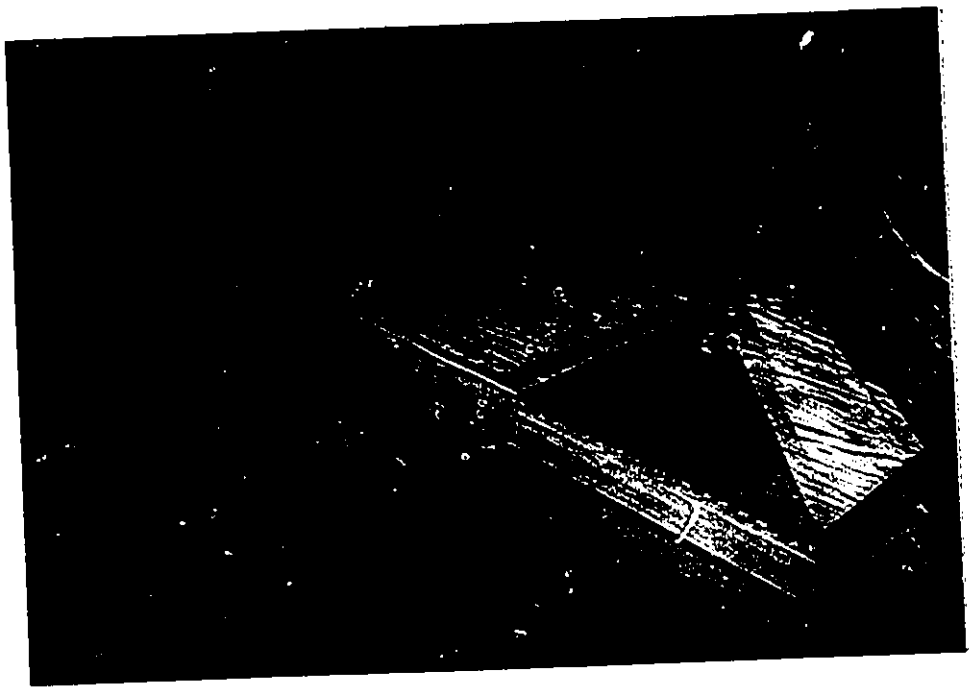

Figure B.3: Model CL

Appendix C

Contour lines of C_p

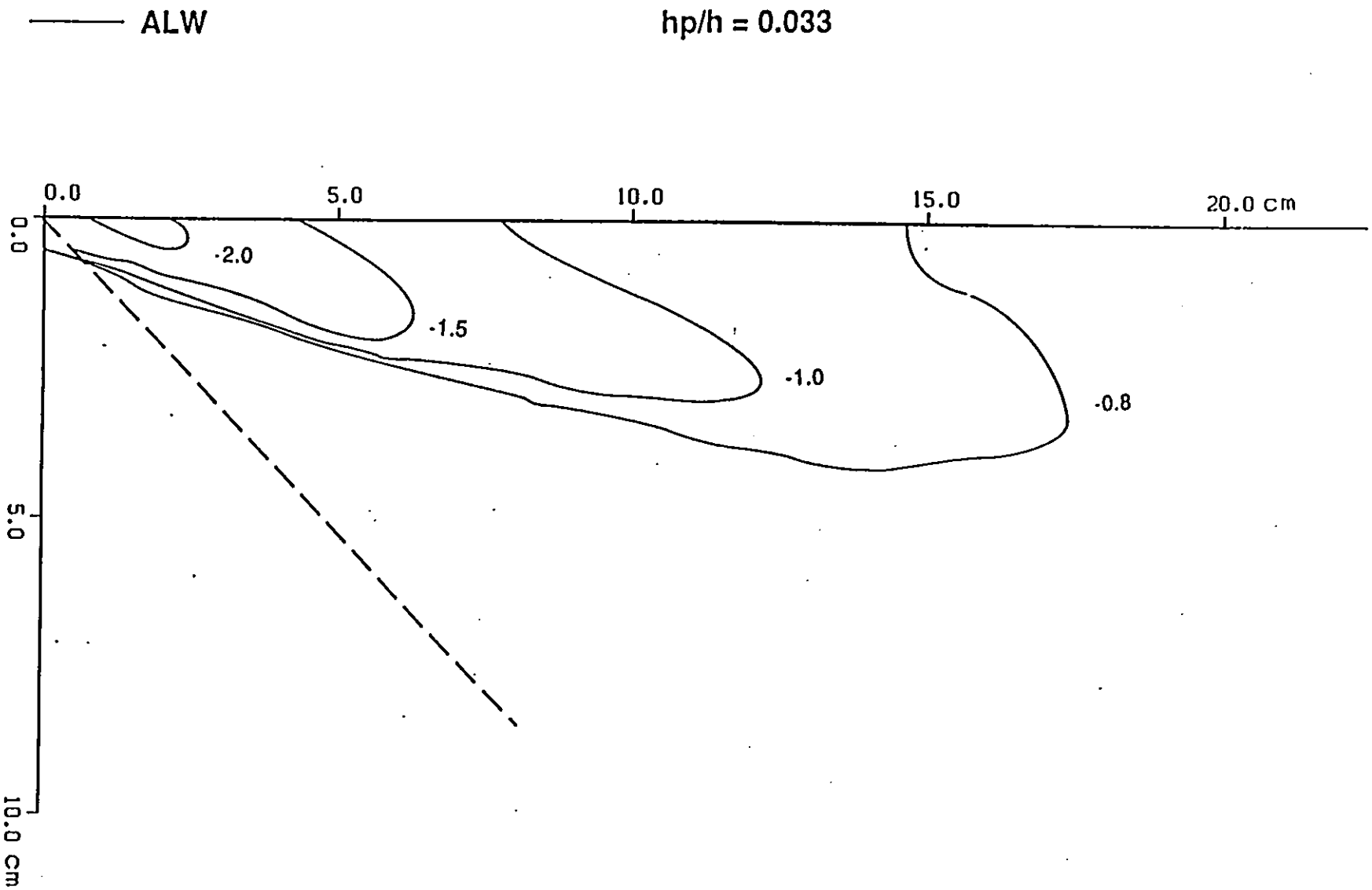

Figure C.1: Mean pressure coefficient : ALW (A ref.)

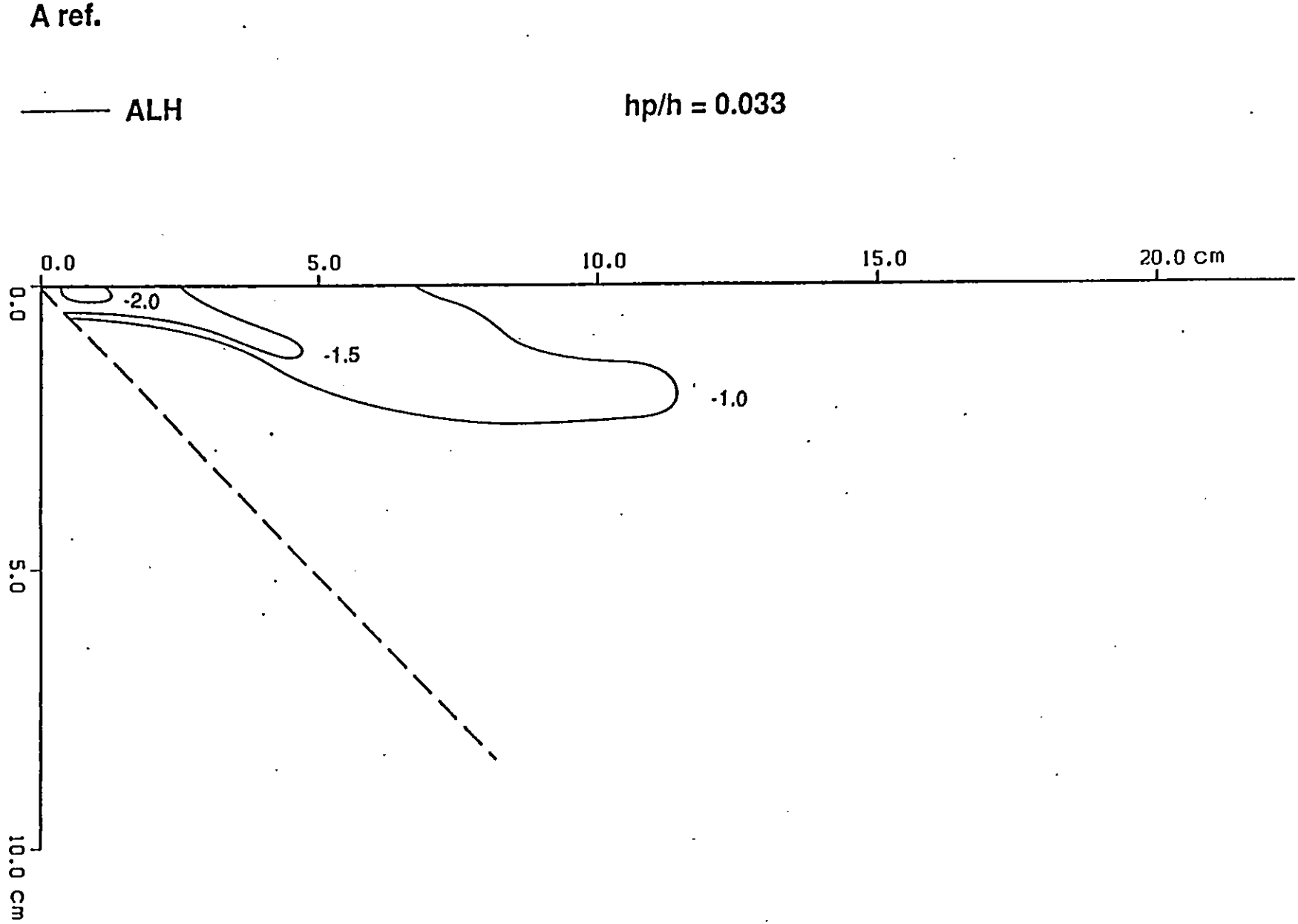

Figure C.2: Mean pressure coefficient : ALH

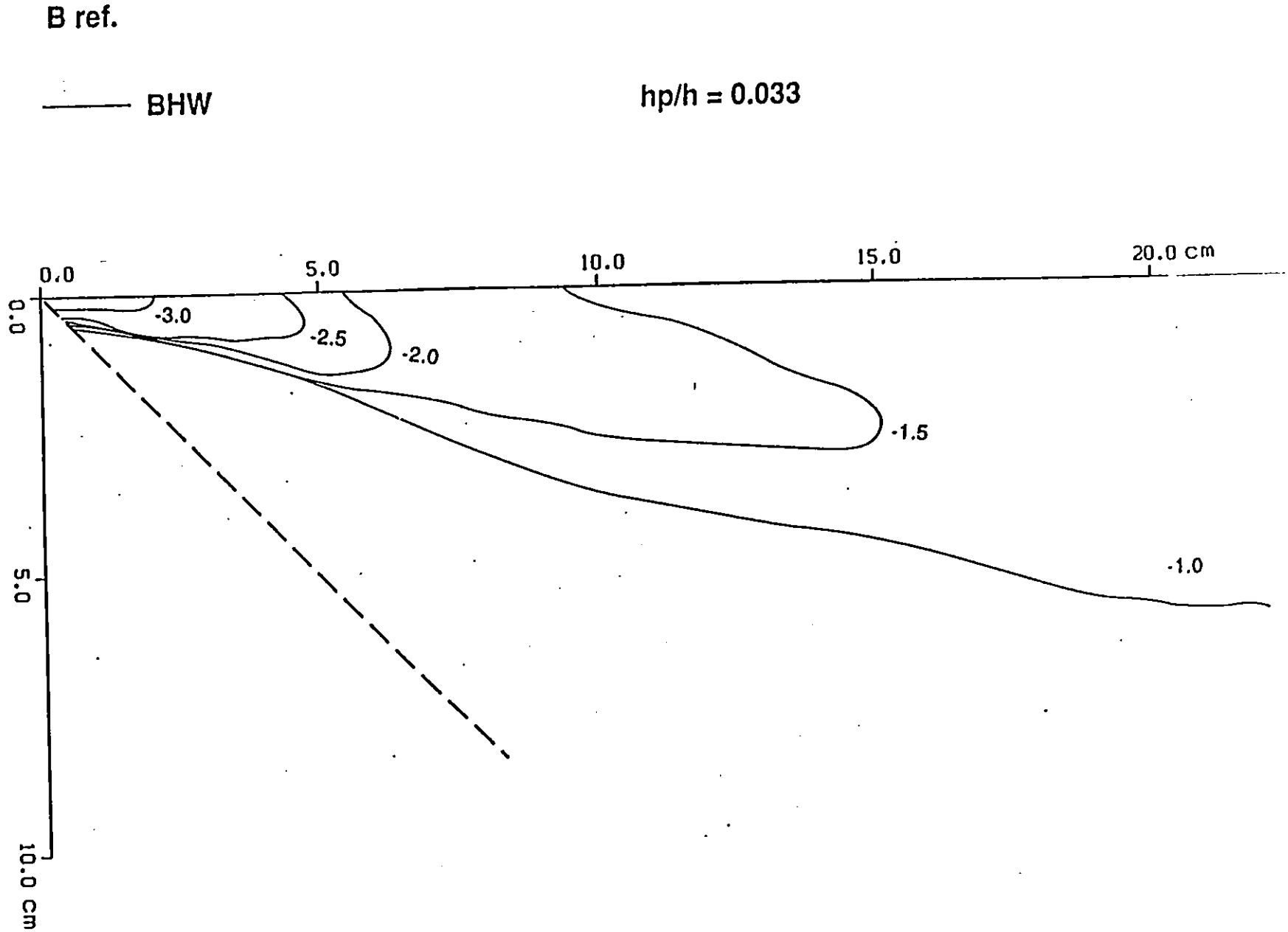

Figure C.3: Mean pressure coefficient : BHW

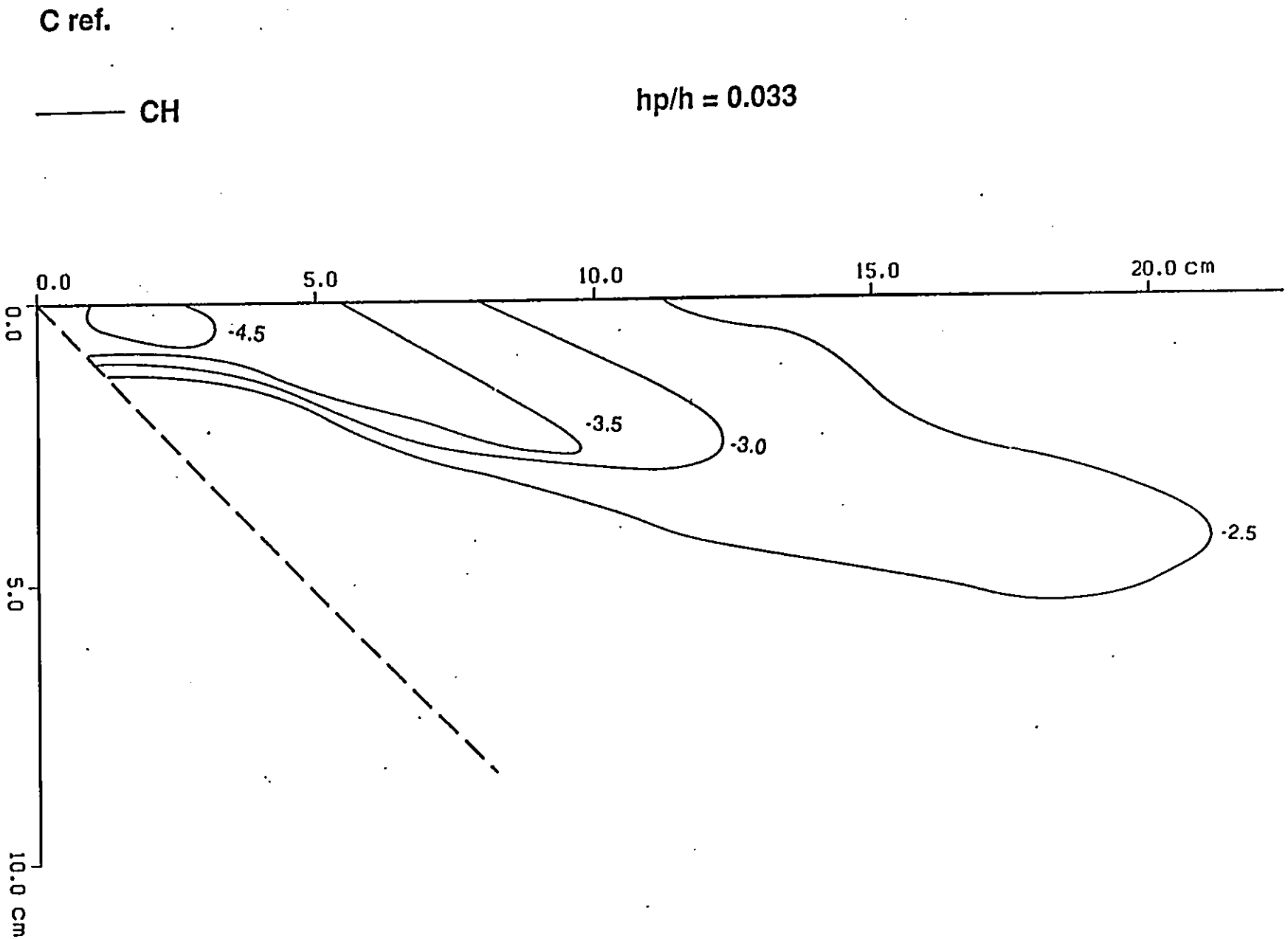

Figure C.4: Mean pressure coefficient : CH (C ref.)

Appendix D

Evaluation of the Exponential Curve

In the section 5.4 of the blockage effect on pressure coefficient, a program on HP 11C calculator was used to determine the best fitting curves.

The curve chosen was an exponential curve defined as $y = ae^{bx}$ to get the closest curve pattern.

From the data points, a and b were determined.

x	$y1$	$y2$	$y3$
1.8	1.86	1.65	1.56
13.4	1.92	1.70	1.60
24.0	3.00	2.75	2.70

After a regression analysis, it was found that :

$$y1 = 1.76e^{0.02x}$$

$$y2 = 1.56e^{0.02x}$$

$$y3 = 1.47e^{0.02x}$$

where x is the blockage ratio and y is the pressure coefficient. The coefficient a of the equation is very close to C_{pc} (the corrected value) and the coefficient b was constant in all three curves and has the value of 0.02. The precision of the curve fitting can be measured by the correlation coefficient r^2 found to be 0.77 in all cases which is quite good since it is close to 1.0.